New field, structural and geochronological data from the Shyok and Nubra valleys, northern Ladakh: linking Kohistan to Tibet

R. F. Weinberg, W. J. Dunlap and M. Whitehouse

Geological Society, London, Special Publications 2000; v. 170; p. 253-275
doi:10.1144/GSL.SP.2000.170.01.14

New field, structural and geochronological data from the Shyok and Nubra valleys, northern Ladakh: linking Kohistan to Tibet

R. F. WEINBERG[1,2], W. J. DUNLAP[1] & M. WHITEHOUSE[3]

[1]*Research School of Earth Sciences, The Australian National University, ACT 0200, Australia*

[2]*Present address: Department of Earth Sciences, Oxford University, Oxford OX1 3PR, UK*

[3]*Museum of Natural History, Stockholm, Sweden*

Abstract: The Nubra–Shyok confluence in northern Ladakh is a key area for understanding the tectonic evolution of NW Himalaya and provides the basis for linking the geology of Pakistan to that of Tibet. The geology of the confluence area has been the subject of much speculation centred mainly on the existence of ophiolites and their regional significance. These ophiolites are thought to represent the eastward extension of the Shyok Suture Zone (SSZ), which separates the Dras island arc from the southern margin of Eurasia, and which was overprinted by movement along the Khalsar Thrust (often thought to represent the eastern continuation of the Main Karakoram Thrust). The geology of the area is relatively complex and the little information available has hampered regional geological correlations.

The Khalsar Thrust (KT) and the dextral Karakoram Fault (KF), two regional tectonic features of NW Himalaya, merge at the confluence defining a triple point and three blocks: the Ladakh block to the south, the Saltoro block to the northwest, and the Karakoram block to the northeast. Close to the triple point, the KF changes strike and movement direction. Movement vector analysis of the triple point indicates that the KT and the two parts of the KF could have moved contemporaneously, and allows prediction of the movement vectors across the faults. The KT and KF shear preferentially volcano-sedimentary rocks of the Shyok and Nubra formations, respectively. Contrary to previous interpretations, these sheared rocks do not represent disrupted ophiolites. Regional tectonic reconstructions, however, require suturing between the Ladakh block and Eurasia and the strike of the SSZ in Baltistan suggests that the suture zone might crop out north of the KT, either along the southern slopes of the Saltoro Range or further north along the Saltoro valley. In the few outcrops of the Saltoro block we were able to visit, we found no evidence of ophiolitic rocks. Instead we found outcrops of the calc-alkaline Tirit batholith. Although our observations do not confirm the presence of the suture-related rocks in the southern Saltoro block, this possibility cannot be ruled out. Zircons from a sample of Tirit granite (U–Pb ion-microprobe age) yielded an age centred at 68 ± 1 Ma. The similar range of modal composition and age of the Tirit and Ladakh batholiths suggest that they are part of the same magmatic event. This result and a number of other observations indicate that the post-75 Ma geology of the Ladakh and Saltoro blocks is similar. Thus, if there is a suture zone in the southern Saltoro block, suturing must have occurred before 75 Ma, as concluded by others along the same tectonic boundary to the west in Pakistan.

The KF represents a much younger terrane boundary, juxtaposing rocks of the Ladakh and Saltoro blocks to those of the Karakoram terrane. Rocks related to suturing of continents were not found along the KF. Karakoram leucogranites cropping out in the southern part of Karakoram terrane yielded a U–Pb zircon age centred at 15.0 ± 0.4 Ma (2σ). Because these leucogranites were not found south of the KF, this fault must have initiated after leucogranite intrusion and must therefore be younger than 15 Ma old. At the confluence the KF cuts across the regional rock sequence than can be followed from Kohistan into Baltistan and into the confluence area. Movement on the fault displaces the sequence by approximately 150 km to southeastern Tibet where the regional rock sequence can be regained.

Correlating the geology of Northern Pakistan to that of western Tibet has been hampered by a relative lack of information in the intervening area in northern Ladakh (India). Northern Ladakh is particularly important for regional correlation because here the regional rock sequence is cut across and displaced by the right-lateral Karakoram Fault (KF), one of the

From: KHAN, M. A., TRELOAR, P. J., SEARLE, M. P. & JAN, M. Q. (eds) *Tectonics of the Nanga Parbat Syntaxis and the Western Himalaya*. Geological Society, London, Special Publications, **170**, 253–275. 1-86239-061-4/00/$15.00

faults controlling the lateral extrusion of Tibet (e.g. Molnar & Tapponnier 1975). Border conflicts have prevented intensive work in the Nubra–Shyok confluence area (from now on referred to as 'the confluence'), which has remained poorly known. In this area the KF intersects (merges with?) the Khalsar Thrust (KT of Srimal *et al.* 1987), which is presumed to have reworked the older Shyok Suture Zone (SSZ). The SSZ separates the Dras island arc to the south, from the Karakoram terrane to the north (Fig. 1; e.g. Coward *et al.* 1986) and is thought to run parallel to the Shyok River in Ladakh (Srimal 1986*a*, *b*). The KT in Ladakh has often been referred to as the eastern continuation of the Main Karakoram Thrust (MKT). West of

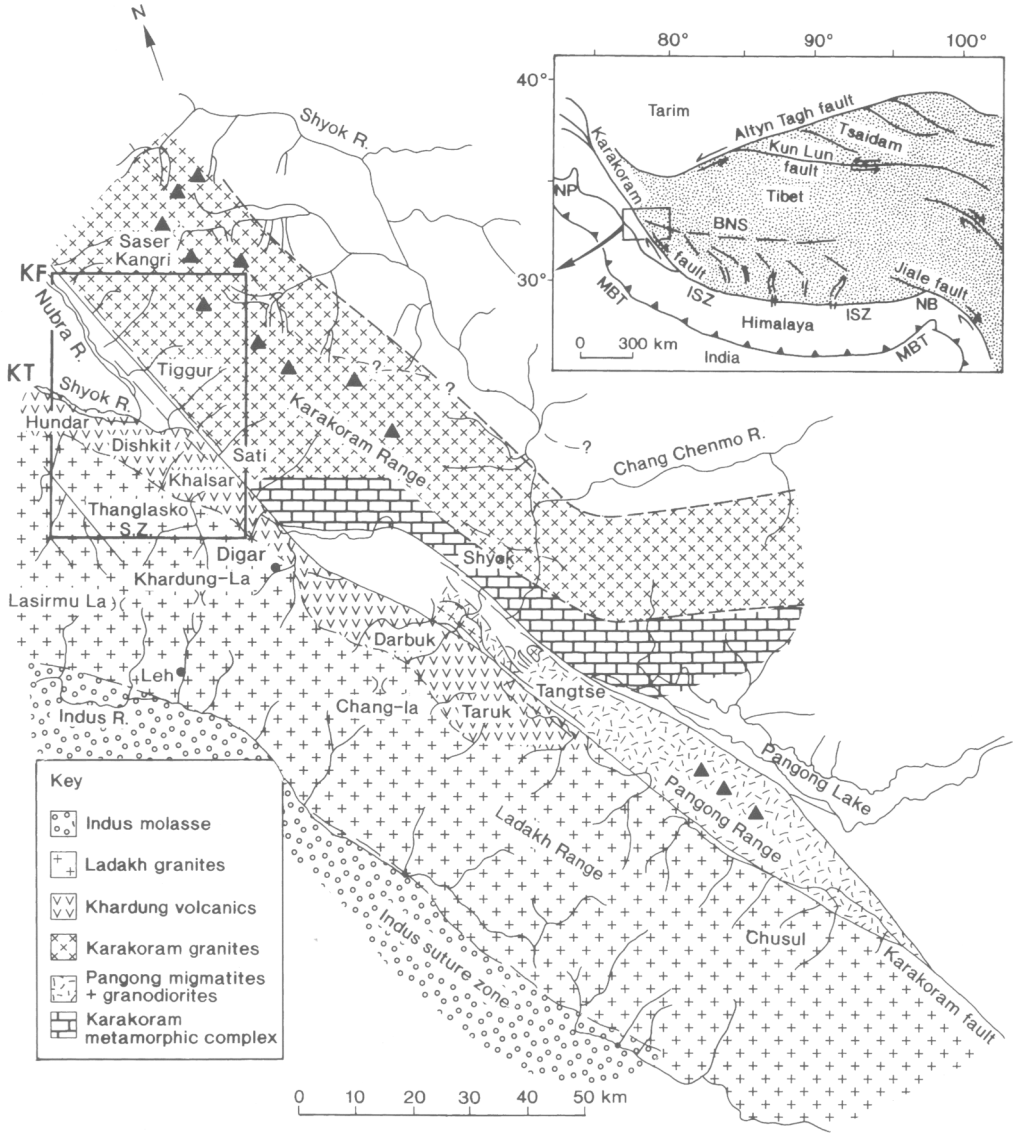

(a)

Fig. 1. (**a**) Regional geological map (after Searle *et al.* 1998). Boxed area marks the Nubra–Shyok confluence area detailed in (b). (**b**) Geological map of the confluence area. Location of samples 711, 021, 95–481 and 95–411 are indicated (95–481 and 95–411 are indicated by numbers 481 and 411, respectively). Inset box shows main tectonic features east and west of the map of the confluence. Legend overleaf.

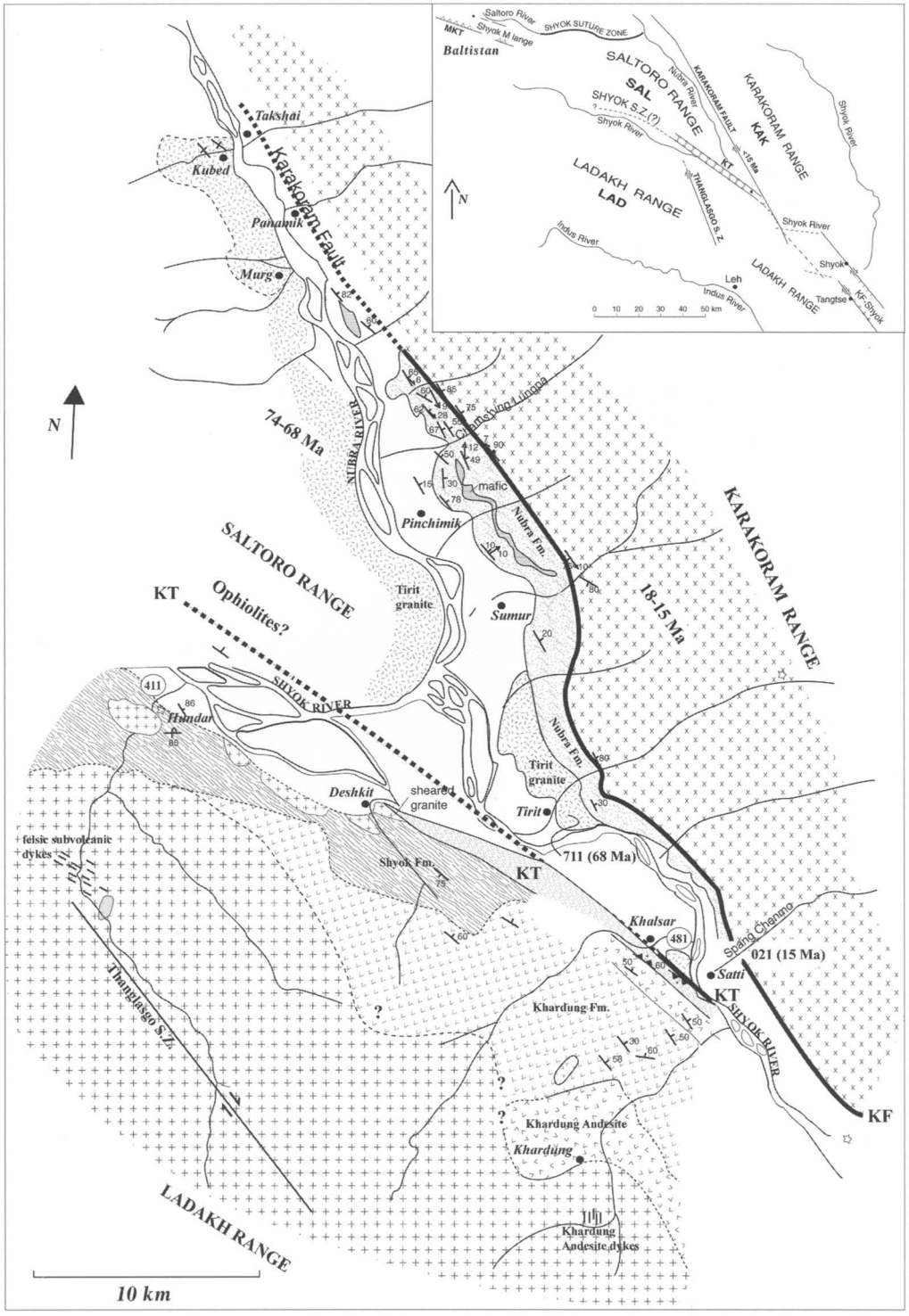
Saltoro River
MKT
Shyok M lange
SHYOK SUTURE ZONE
Baltistan
SALTORO RANGE
SAL
SHYOK S.Z.(?)
Nubra River
KARAKORAM FAULT
KARAKORAM RANGE
KAK
Shyok River
KT
~15 Ma
LADAKH RANGE
LAD
THANGLASGO S.Z.
Indus River
Leh
Tangtse
KF-Shyok
0 10 20 30 40 50 km
N
Takshai
Kubed
Panamik
Murg
Karakoram Fault
74-68 Ma
NUBRA RIVER
Changlung Lungpa
mafic
Pinchimik
Nubra Fm.
SALTORO RANGE
KT
Ophiolites?
Tirit granite
Sumur
18-15 Ma
KARAKORAM RANGE
411
Hundar
SHYOK RIVER
Deshkit
sheared granite
Tirit
Tirit granite
Nubra Fm.
felsic subvolcanic dykes
Shyok Fm.
711 (68 Ma)
KT
Khalsar
481
Spang Chenpo
021 (15 Ma)
Satti
KT
SHYOK RIVER
Khardung Fm.
Thanglasgo S.Z.
Khardung Andesite
Khardung
KF
LADAKH RANGE
Khardung Andesite dykes
10 km

(b)

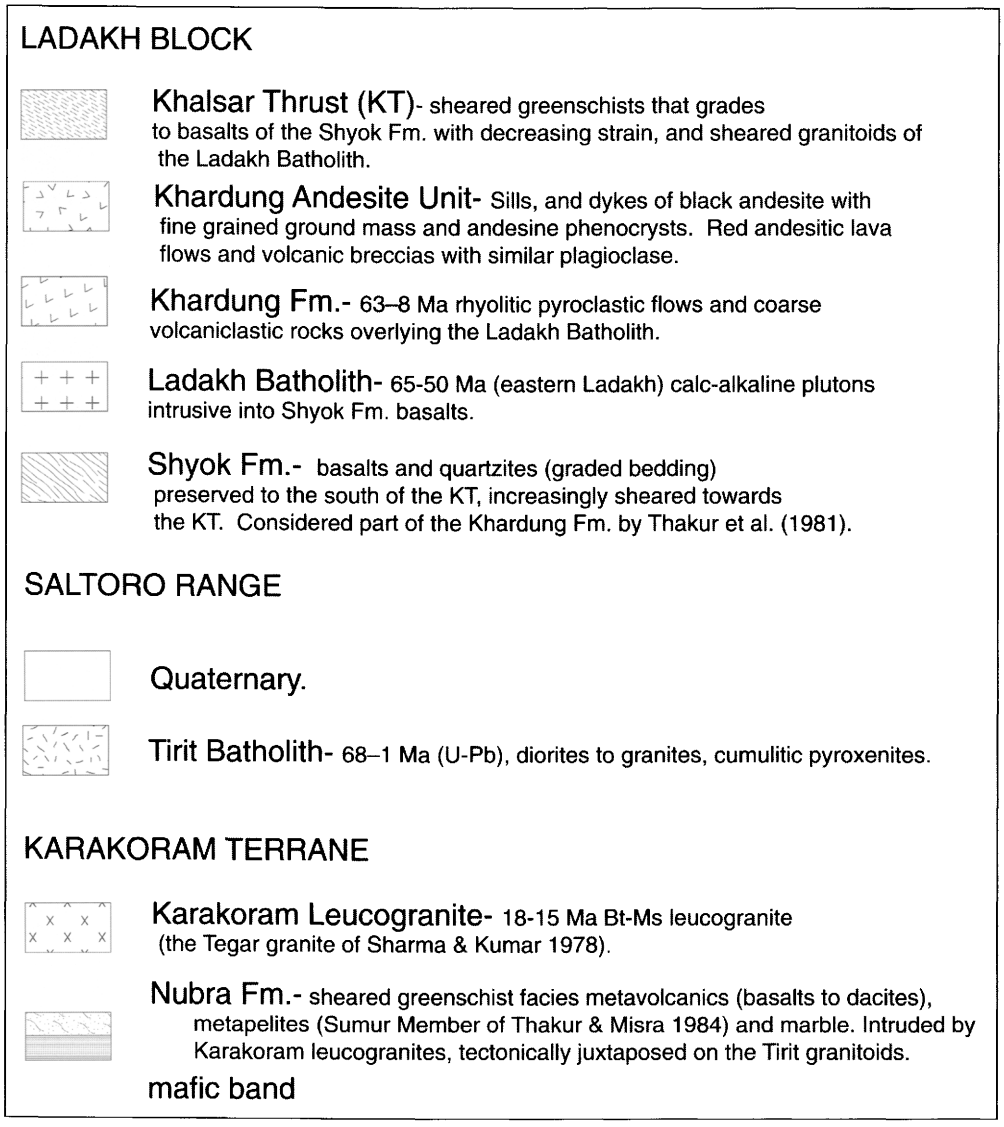

Fig. 1(b) Cont.

Ladakh the MKT reworks the SSZ and follows it along the northern boundary of the Dras island arc, continues west undeflected by the Nanga Parbat–Haramosh spur, and onward to Kohistan where it defines the northern boundary of the Kohistan arc (where it was previously known as the Northern Suture Zone). The Ladakh and Kohistan blocks are bounded to the south by the Indus Suture Zone, and it has been suggested that these two arcs represented a single island arc which collided with the southern margin of Eurasia before India collided with the system (Petterson & Windley 1985; Coward *et al.* 1986; Pudsey 1986; Searle 1991). Despite some doubts raised by Raz & Honegger (1989) on whether the Ladakh batholith developed within a pure island arc (Dras) or a transition between continental and island arc, we prefer the interpretation that Ladakh was an island arc. This is because, unlike the Lhasa block to the east where a Precambrian basement and Mesozoic cover has been found (Allègre *et al.* 1984), no evidence has been found of an older continental basement (see Honegger *et al.* 1982; Weinberg & Dunlap in press and references therein).

Published descriptions and maps of the Nubra–Shyok confluence differ widely and are often contradictory (e.g. Sharma & Kumar 1978; Thakur *et al.* 1981; Rai 1982; Thakur & Misra 1984; Srimal 1986*a*, *b*; Srimal *et al.* 1987). A clear picture of the geological evolution of the confluence has therefore not yet emerged. Despite its obvious importance, the Shyok–Nubra confluence remains relatively poorly known. Several explorers studied the geology of the confluence area and the Pangong lake area late last century and early this century (Hedin 1907; de Terra 1932; Dainelli 1933–1934). After 1939 and later partition between India and Pakistan, very few workers covered this area until the 1970s, when a number of Indian workers started to explore the confluence area. It was only in early 1994 when the Shyok and Nubra valleys were reopened to foreigners. Access remains limited to certain areas along the Nubra and Shyok valleys (excluding the entire Saltoro Range) and to visits not exceeding one week. This work is a result of our observations during six short trips to the area, over three field seasons. We aimed at understanding the relationship between the suture zone and the KT and KF, which merge at the confluence, and to link the geology of the confluence to that of Baltistan (area immediately west of Ladakh in Pakistan); and Kohistan and to that of western Tibet, across the KF. Here, we describe our field observations as well as new U/Pb zircon ages and Ar/Ar cooling ages of key samples. After describing the regional geology we describe our observations on the geology of the confluence in three parts, corresponding to three main geological blocks defined by the KT and KF. We then describe our geochronological results, followed by structural analysis.

Regional geology

The Shyok Suture Zone (SSZ) north of the Ladakh batholith was first described by Gansser (1980) and later by others (Tahirkheli *et al.* 1979; Brookfield & Reynolds 1981; Rai 1982; Thakur & Misra 1984; Srimal 1986*a*, *b*; Hanson 1989; Brookfield & Reynolds 1990; Allen & Chamberlain 1991; Lemennicier *et al.* 1996). Based on the little available information, the main trace of the suture zone has been placed either north of the Saltoro Range along the Saltoro River (Gansser 1980), or more commonly along the Shyok River, south of the Saltoro Range (Fig. 1b insert; e.g. Srimal 1986*a*, *b*). In Kohistan, the SSZ represents the remains of a small back-arc basin that separated the Kohistan–Dras island arc and Asia (Pudsey 1986), which closed in the early late Cretaceous (100–85 Ma e.g. Treloar *et al.* 1989, 1996). Hanson (1989) described in detail the SSZ in the Shigar valley, Baltistan, where it is defined by a simple fault and a few pods of serpentinite of ultramafic origin, separating Paleozoic sedimentary rocks of the Eurasian plate from Cretaceous rocks of the Dras island arc. The presence in Shigar of marine sediments of Cretaceous age suggests a small ocean basin between the two terranes. Brookfield & Reynolds (1990) described in detail the SSZ near the confluence of the Hushe and Saltoro rivers, 100 km west of the Nubra–Shyok confluence area (insert on Fig. 1b). They mapped a tectonic mélange, defining a flower structure, separating Asian rocks from Ladakhi rocks, which may contain ophiolitic units (Coward *et al.* 1986). The geology of the intervening 100 km between the Hushe–Saltoro and the Nubra–Shyok confluences is virtually unknown.

In Baltistan, the Main Karakoram Thrust (MKT) runs approximately N60W along the Shyok valley, and has reworked the SSZ and thrusted Karakoram terrane onto Ladakh terrane (Tahirkheli *et al.* 1979; Coward *et al.* 1986; Searle *et al.* 1989; Allen & Chamberlain 1991). The eastward continuation of the MKT into Ladakh remains unknown. The 700 km long dextral Karakoram Fault (KF) runs through the Nubra and upper (eastern) Shyok valleys, striking N30W to N45W. East of the Nubra–Shyok confluence it separates rocks of the Ladakh terrane from those of the Karakoram terrane (Searle *et al.* 1998). It has been suggested that the KF marks the southern boundary of the Tibetan block, and that together with the sinistral Altyn Tagh Fault, it has accommodated 1000 km of eastward extrusion of the Tibetan Plateau (e.g. Peltzer & Tapponnier 1988). Searle *et al.* (1998), however, determined that the fault is a relatively young structure (<18 Ma) with a maximum dextral displacement of less than 150 km. Rocks southeast of the Pangong Lake in western Tibet define a suture zone, on the east side of the KF, which can be traced all the way to Amdo, 1200 km to the east, defining the Pangong–Nujiang Suture Zone, separating the Changtang and Lhasa blocks (e.g. Allègre *et al.* 1984; Ratschbacher *et al.* 1994). This suture zone has been tentatively related to the SSZ (Searle 1996).

The Ladakh and Karakoram batholiths underlie the two main mountain ranges near the confluence (Fig. 1a). The Ladakh batholith and its extrusive equivalents—the Khardung Fm. (e.g. Srimal 1986*a* and Srimal *et al.* 1987)—are part of the 2500 km long Trans-Himalayan igneous belt, a pre-collisional calc-alkaline belt (e.g. Honegger *et al.* 1982). The batholith was active between 102 ± 2 Ma and 50 ± 1 Ma

(Honegger *et al.* 1982; Schärer *et al.* 1984; Weinberg & Dunlap in press). Three rocks dated close to the confluence area yielded U–Pb zircon crystallization ages between 65 and 50 Ma (Weinberg & Dunlap in press). The Karakoram batholith is a 700 km long arcuate body, composed of older, mid-Cretaceous and Palaeocene–Eocene calc-alkaline plutons, and a distinctive Miocene peraluminous leucogranite suite which originated from widespread crustal anatexis during continental collision (Searle *et al.* 1992). The post-collisional Baltoro Plutonic Unit is the main component of the Karakoram Range in Pakistan. It has U–Pb zircon ages of 21.0 ± 0.5 Ma (Parrish & Tirrul 1989) and monazite ages of $25.5^{+0.3}_{-0.6}$ Ma (biotite leucogranite) and $21.4^{+0.3}_{-0.8}$ Ma (two-mica garnet leucogranite; Schärer *et al.* 1990). These ages are somewhat older than the 18.0 ± 0.6 Ma Karakoram (Tangtse) leucogranite, cropping out some 120 km SE of the confluence (Searle *et al.* 1998).

In between the Ladakh and Karakoram batholiths, volcano-sedimentary rocks have localized deformation. These rocks were divided by Thakur & Misra (1984) into the Shyok and Nubra groups. According to these authors, the Shyok Group consists of dismembered fragments of an ophiolite sequence comprising basic and intermediate volcanic rocks, together with chert, gabbro, peridotite and serpentinite interbedded with phyllite, slate, limestone and quartzite. Their Nubra Group, cropping out along the Nubra River, consists of sandstone, conglomerates and shale interbedded with basic volcanic, serpentinite, pyroxenite and garnet–mica schist. Srimal (1986*b*) and Srimal *et al.* (1987) mapped the Saltoro Range, between the Nubra and Shyok valleys. They found two ophiolitic sequences, one to the south which they called the Biagdang ophiolite, cropping out on both sides of the Shyok River, and the other on the northeastern slopes of the Saltoro Range, which they called the Saltoro ophiolite. Several maps of the confluence area indicate the presence of granites between the KT and the KF close to Tirit and in the Saltoro Range (Tirit batholith; e.g. Thakur & Misra 1984; Srimal *et al.* 1987). We have found no evidence of peridodites, nor of any sheared or deformed ultramafic rocks, and our observations and interpretations broadly disagree with those of previous authors.

Geology of the Shyok–Nubra confluence

The main geological and tectonic features of the confluence area, and the known ages are summarized in Figs 1 and 2. Our observations extend from Khardung in the south to Panamik and Kubed in the north, and from Hundar in the west to SE of Satti. The Khalsar Thrust (KT) and the Karakoram Fault (KF), define a triple point at their intersection at the confluence and separate three blocks: the Ladakh (LAD), the Saltoro (SAL) and the Karakoram (KAK) blocks (insert on Fig. 1b).

Ladakh block and Khalsar Thrust (KT)

The Ladakh block lies south of the KT and KF. It is characterized by granitoids belonging to the Ladakh batholith intruding an older sequence of basalts and quartzites—the Shyok Formation—and overlain by pyroclastic flows of the Khardung Formation. The Shyok Fm. is well preserved near Hundar where it consists of folded basaltic flows interlayered with narrow (0.5–1 m) bands of sandstone. The presence of graded-bedded sandstone suggests that the basalts are not part of an ophiolitic sequence, but more likely part of the Dras island arc. Thakur *et al.* (1981) mention a Lower Cretaceous age for the Shyok Fm.

The Ladakh batholith has been described in a number of papers (e.g. Honegger *et al.* 1982; Weinberg & Dunlap in press) and will not be further described here. The 63 ± 8 Ma (Srimal *et al.* 1987) calc-alkaline Khardung Fm. are the extrusive equivalent of the Ladakh batholith. It is a thick sequence of felsic pyroclastic flows with angular blocks of various volcanic, plutonic and sedimentary rock types, interlayered with coarse volcaniclastic rocks. Its thickness varies considerably along strike (*c.* 5 km at Khardung) from Hundar in the west to Chushul 200 km east. These flows now generally dip 30–60° NE, suggesting post-depositional tilting. The original contact between the Shyok Fm. and the younger Khardung Fm. is obscured by deformation and thrusting along the KT, but it was most likely an unconformity. The contact between the Khardung Fm. and Ladakh granitoids at Khardung is intruded by a large andesite sill which is linked to dykes intruding the underlying granitoids and the overlying Khardung Fm., where they feed smaller sills. This andesite extruded on top of the Khardung Fm., giving rise to a red andesite lava flow. The main sill at Khardung is 2 km wide, and its contact with the underlying granite dips roughly 40–50° NE. These andesitic rocks—which we called the **Khardung Andesite Unit**—are clearly younger and more mafic than the Khardung Fm.

Between Hundar and Deshkit, basalts of the Shyok Fm. and intrusive Ladakh granitoids become increasingly sheared and retrograded to

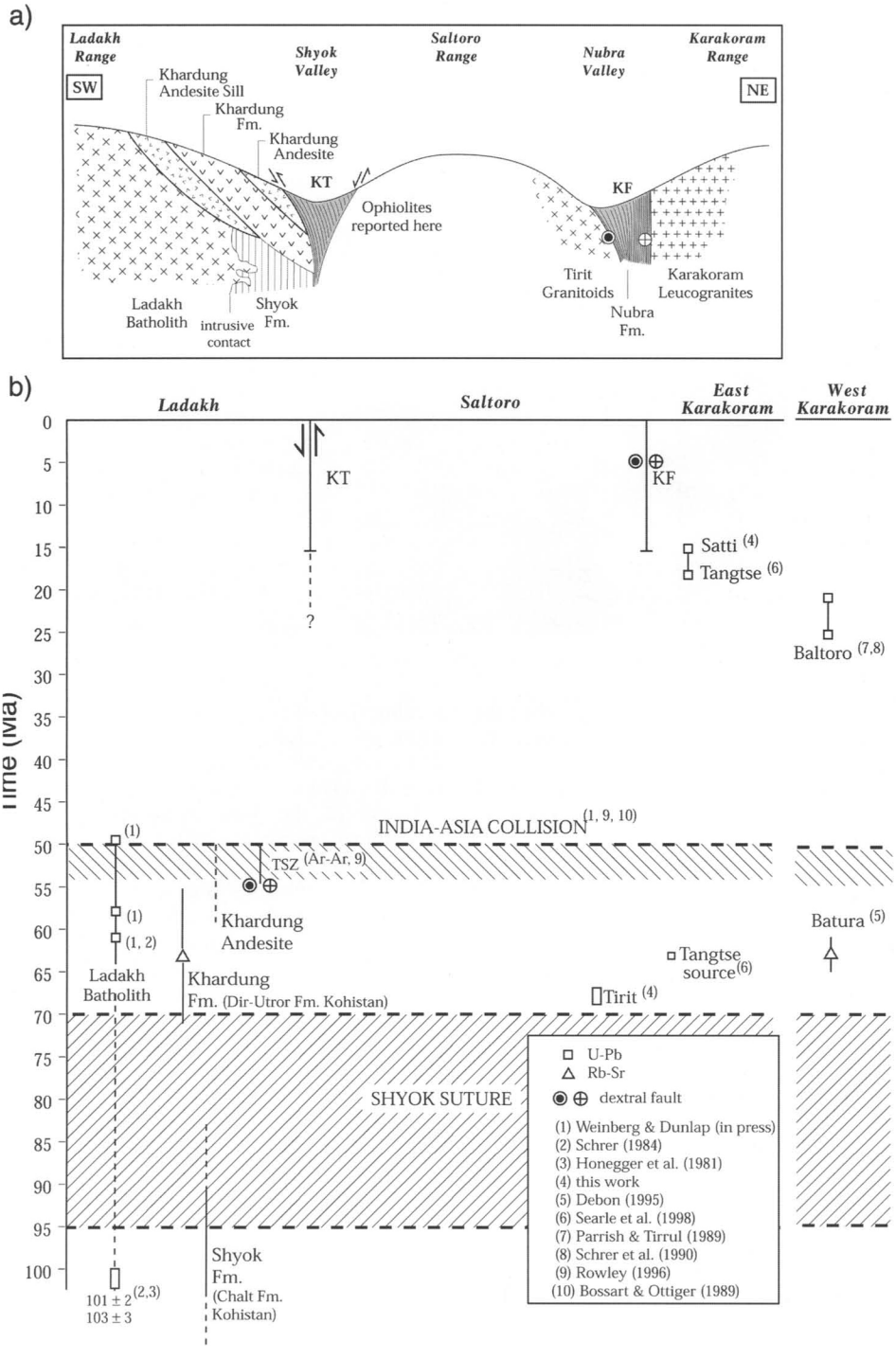

Fig. 2. (**a**) Schematic geological profile across the northern Ladakh Range, the Saltoro Range and the southern Karakoram Range, summarizing our observations. (**b**) Summary of measured and estimated ages of rocks and structures in northern Ladakh, and the Karakoram Range. The Nubra Fm. is not shown and has an estimated Permian age.

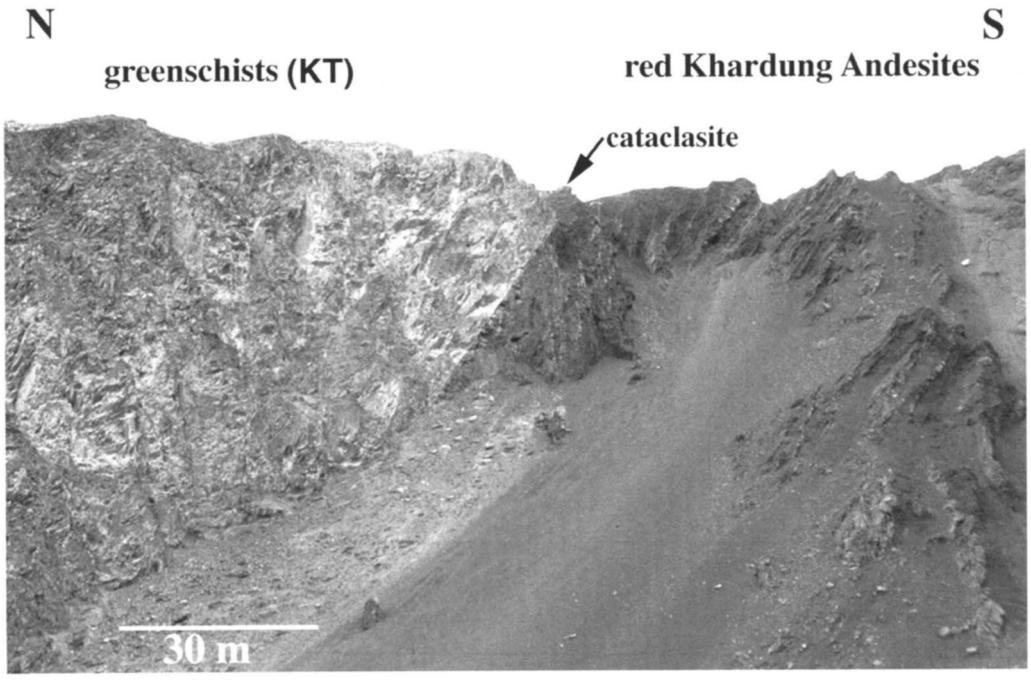

Fig. 3. The Khalsar Thrust (KT) at Khalsar.

greenschist facies as a result of shearing along the KT (Fig. 1). The KT is best exposed between the villages of Deshkit and Khalsar. It is a zone several hundred metres wide and exposures at Khalsar indicate south-directed thrusting (Fig. 3) in accordance with down-dip lineation and kinematic indicators (see the 'Structural analysis' section). Thakur *et al.* (1981) divided the geology into groups based on the deformation state of the rocks. Thus, they joined undeformed or weakly deformed rocks, basalts and quartzites of the Shyok Fm., and younger pyroclastic flows of the Khardung Fm. under the term 'Khardung volcanics'. Sheared greenschists of the Shyok Fm. were separated from preserved basalts of the same formation, and were called the 'Khalsar Member'.

Saltoro block

The Saltoro block forms a wedge north of the KT and west of the KF (Fig. 1b). The most detailed work in the Saltoro Range was that by Srimal (1986*a*, *b*), who described a 7.5 km thick ophiolitic sequence of basic rocks on the south Saltoro Range (the Biagdang ophiolite). These rocks are intruded by granitoids, just as the Shyok Fm., and metamorphosed mainly at greenschist facies (Srimal 1986*a*). Most of the Saltoro block is out of bounds for travellers, but we were nevertheless able to study outcrops of this block in three localities, all of which were located immediately south of the KF and exposed plutonic rocks, collectively referred to as the Tirit batholith (Fig. 1b; Thakur *et al.* 1981).

Rocks of the Tirit batholith are exposed immediately north of the KT, near Khalsar. It is represented by a medium-grained, weakly deformed hornblende diorite, with labradorite and minor biotite (Ar–Ar sample 95–481, below). The Tirit batholith also crops out near Tirit village, directly underlying the mylonitic sedimentary rocks of the Nubra Fm. Here, granitoids are altered and fractured, and two thin sections of augite–hornblende tonalites and one of felsic granite showed rocks intensely fractured but with no signs of plastic deformation, suggesting cold deformation ($T < 300$–$250\,^{\circ}C$). This contrasts with ductile mylonites of Karakoram leucogranite found within the KF, only a few hundred metres across strike. Sheared Tirit batholith rocks crop out in the Saltoro mountains close to the village of Kubed. We inspected an estimated 4 km across strike, and found sheared plutonic rocks retrogressed in greenschist facies conditions but locally preserving intrusive relationships. In thin sections these rocks are recrystallized and composed mostly of metamorphic minerals. The Nubra valley trends at a small angle to the strike of the foliation in these rocks (N40–60W), and sheared granitoids

crop out along the lower slopes of the Saltoro Range, all the way south to the confluence at Tirit (see Srimal 1986*a*). Morainic and alluvial blocks carried down the Kubed valley are of plutonic rocks (no sedimentary blocks found), mostly unaltered, undeformed gabbros and diorites, coarse cumulitic pyroxenites, and granites and granodiorites, and only a few gneisses. All blocks observed were typical of calc-alkaline sequences, such as the Ladakh batholith, and not related to an ophiolite, as interpreted by Srimal (1986*a*, *b*, 1987; their Saltoro ophiolite).

Karakoram block and Karakoram Fault (KF)

Three rock sequences crop out in the Karakoram Range: the Nubra Fm. (Thakur & Misra 1984), the Karakoram leucogranite batholith (the Baltoro Plutonic Unit in Pakistan) and an older I-type granitoid belt (Srimal *et al.* 1987). The I-type belt crops out in the most remote part of the batholith and was not covered by this work. The Nubra Fm. is a rock sequence *c.* 1–2 km wide cropping out along the foot of the Karakoram Range, between the Tirit batholith and Karakoram leucogranite. It is comprised of metavolcanic and metapelitic rocks metamorphosed to green, grey and black schists and sheared by movement on the KF. Primary structures are preserved locally such as in an outcrop of porphyritic andesite lava breccia (isolated outcrop south of Panamik; Fig. 1b). Metadacites, now metamorphosed to greyschists, preserve primary plagioclase and quartz phenocrysts in a felsic matrix. Common greenschists are composed of actinolite–chlorite–epidote–carbonate–plagioclase–quartz and were most likely originated from metamorphism of basic rocks. Some of these greenschists also have dark green tourmaline aggregates or single crystals up to 5 mm long. Grey and black Bt–Ms–Chl schists with fine felsic and mafic bands were interpreted as metapelites. In one metapelite sample we found sericitized pseudomorphs of cordierite, 1 cm in diameter, which suggests that the Nubra Fm. attained hornblende hornfels facies (Cd + Bt + Ms paragenesis) before greenschist facies retrogression. We report also marble occurrences, in the Sumur Gorge (muddy and sheared carbonates), near Satti and Rongdu (brown folded marble layers).

The presence in the Nubra Fm. of mylonitic leucogranite layers up to tens of metres wide and locally cross-cutting the foliation, particularly

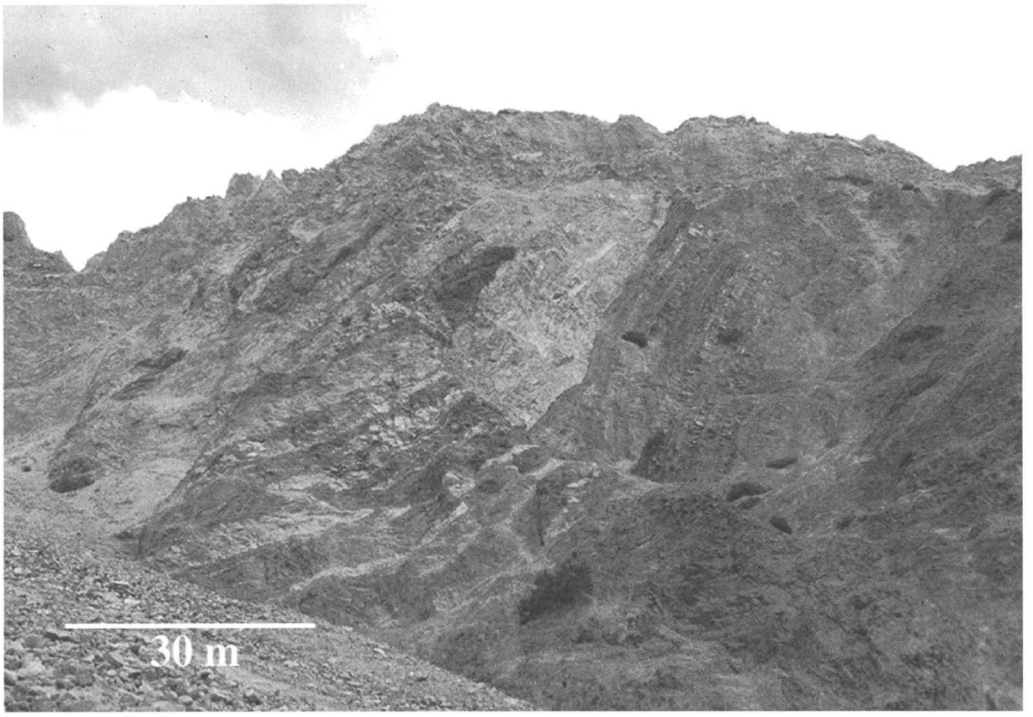

Fig. 4. Intrusive contact between the Karakoram leucogranite (left-hand side) and the Nubra Fm. (right-hand side) near Pinchimik. Note intrusive dykes folded within the Nubra Fm.

close to the contact with the Karakoram leucogranite (Fig. 4), suggest that the Nubra Fm. was the wall rock of the Karakoram batholith and therefore part of the Karakoram terrane. The Nubra Fm. has taken up most of the strain due to movement on the KF. Strain intensity varies across the sequence but generally increases gradually towards the contact between the Nubra Fm. and Karakoram leucogranite where it is characterized by a band of mylonites of *c.* 200–400 m shearing both sides of the contact (see the 'Structural analysis' section). North of the contact mylonites, the Karakoram batholith is composed mainly of Bt–Ms leucogranite with minor Ms leucogranite (the Tegar granite of Sharma & Kumar 1978). We explored 10 km up the Spang Chenmo valley, north of Satti, and up the Rongdu valley to the east, where the batholith is very homogeneous, comprised of massive Bt–Ms leucogranite, with some sedimentary xenoliths but no mafic enclaves. Quartz has been deformed plastically and feldspar grains are fractured. Igneous muscovite comprises up to 2–3% (modal) of the rock. We noted a variety of blocks in the scree coming down from the Karakoram Range, including sheared dolomitic breccia, white marble, black andalusite schist and granodiorite with mafic enclaves (probably part of the older I-type granitoids described by Srimal *et al.* 1987).

In summary, the Nubra Fm. is a sequence of multicoloured schists resulting from greenschist facies metamorphism of basalts, andesites, dacites, pelitic rocks and marble, later intruded by Karakoram leucogranite. The Karakoram Fault shears most of the Nubra Fm., but shearing is concentrated to a 200–400 m wide band of mylonites along the contact with the Karakoram leucogranite.

Geochronology

In order to further constrain the geological history of the confluence area we determined the crystallization age of zircons from two granite samples (Tables 1 and 2) and the Ar–Ar cooling histories of two other samples (Tables 3 and 4).

Tirit batholith—U–Pb and Ar–Ar

We carried out U–Pb dating of zircons from a tonalite sample collected at Tirit (sample 96–711) and Ar–Ar analysis of hornblende grains of sample 95–481. Sample 96–711 has no signs of plastic deformation, but was altered and fractured, with plagioclase partly altered to sericite and calcite, undeformed quartz, green to transparent amphibole, and transparent pyroxene, as well as opaque grains, chlorite and epidote. U–Th–Pb analyses were performed using a Cameca ims1270 ion-microprobe at the Swedish Museum of Natural History, Stockholm (Nordsim facility) following analytical methods described by Whitehouse *et al.* (1997) and Zeck & Whitehouse (in press). U/Pb and Th/Pb ratios are calibrated relative to the 1065 Ma Geostandards zircon 91500 (Wiedenbeck *et al.* 1995). The accuracy of $^{206}Pb/^{238}U$ ages from young zircons

Table 1. *Ion-microprobe (Cameca ims 1270) U–Th–Pb data for zircons from 96–711 (Tirit granite)*

Spot	Date	U (ppm)	Th (ppm)	%co ^{206}Pb	$^{207}Pb/^{206}Pb$	$^{232}Th/^{208}Pb$	$^{238}U/^{206}Pb$	$^{208}Pb/^{232}Th$ age (Ma)	$^{206}Pb/^{238}U$ age (Ma)
5a	1	238	299	1.30	0.0501 ± 27	335 ± 25	93.6 ± 0.8	60.3 ± 4.9	68.5 ± 0.6
4a	1	357	317	0.65	0.0497 ± 19	331 ± 25	93.4 ± 0.8	61 ± 5	68.6 ± 0.6
8a	1	686	1226	0.65	0.0469 ± 13	316 ± 23	93.4 ± 0.8	63.8 ± 5	68.7 ± 0.6
7a	1	511	775	0.14	0.0461 ± 16	333 ± 25	94.7 ± 0.8	60.6 ± 4.9	67.7 ± 0.6
6a	1	321	304	0.57	0.0492 ± 20	328 ± 25	93.6 ± 0.8	61.5 ± 5.1	68.5 ± 0.6
1a	1	127	109	0.83	0.0456 ± 31	309 ± 25	91.2 ± 1.5	65.2 ± 5.7	70.3 ± 1.2
2a	1	117	100	0.46	0.0449 ± 39	298 ± 24	93.6 ± 1.5	67.7 ± 5.9	68.5 ± 1.1
3a	1	161	111	1.34	0.0502 ± 31	324 ± 26	95.9 ± 1.5	62.3 ± 5.4	66.9 ± 1.0
99a	1	416	468	0.38	0.0467 ± 19	319 ± 24	90.7 ± 1.1	63.2 ± 5.1	70.7 ± 0.8
10a	2	138	82	9.13	0.0961 ± 59	393 ± 42	95.3 ± 2.8	51.4 ± 6.1	67.3 ± 2.0
10b	2	135	105	0.23	0.0501 ± 21	284 ± 18	95.9 ± 2.9	71 ± 4.8	66.8 ± 2.0
12a	2	95	79	3.80	0.0497 ± 32	543 ± 53	112.6 ± 4.9	37.2 ± 4	57.0 ± 2.5
11a	2	493	909	2.32	0.0614 ± 20	324 ± 18	101.4 ± 2.7	62.3 ± 3.7	63.2 ± 1.7
13a	2	204	213	0.97	0.0508 ± 17	331 ± 19	98.4 ± 2.4	61 ± 3.7	65.2 ± 1.6
14a	2	200	225	6.95	0.0546 ± 22	567 ± 42	114.5 ± 4.1	35.6 ± 2.8	56.1 ± 2.0
5b	2	176	204	4.07	0.0568 ± 21	359 ± 27	102.7 ± 3.2	56.3 ± 4.6	62.5 ± 2.0
9a	1	113	104	0.00	0.0523 ± 34	317 ± 25	93.2 ± 1.6	63.8 ± 5.4	68.8 ± 1.2

Season date: 1 04/02/98
2 08/02/98

based upon this calibration has been tested by analysis of zircons from a volcanic tuff at Possagno, Italy: conventional measurements of these zircons have yielded 35.5 ± 0.1 Ma (Fischer *et al.* 1989; F. Oberli, pers. comm.), and ion probe measurements yielded 35.1 ± 2.2 Ma (2σ; S. Nicolescu, pers. comm.). The zircons in this study are too young to yield reliable $^{207}Pb/^{206}Pb$ ages because of the large errors associated with measuring very small ^{207}Pb peaks. Th/Pb ages are similarly affected by possible systematic errors in centring of a very small ^{208}Pb peak and are consistently lower than $^{206}Pb/^{238}U$ ages. Common Pb corrections, based upon present-day (Stacey & Kramers 1975) terrestrial Pb are generally *c.* 1% of ^{206}Pb or less (see Table 1).

The results are shown in Fig. 5 and Table 1. Fourteen analyses yielded a group of $^{206}Pb/^{238}U$ with a weighted mean average of 68 ± 1 Ma (2σ). A chi square test resulted in over 99% likelihood that the results belong to the same age group ($\chi^2 = 2.99$ for 13 degrees of freedom). Four points were excluded from the final data analyses (spots 10a, 12a, 14a and 5b) because they had $^{206}Pb/^{238}U$ ages different from the main group, very large common lead corrections (of over 3%,

Table 2. *Zircon U–Pb SHRIMP II analyses of Sample 021 (Satti leucogranite)*

Spot	Date	Core 1 rim 2	U (ppm)	Th (ppm)	%co ^{206}Pb	%co ^{208}Pb	$^{207}Pb/^{206}Pb$	$^{238}U/^{206}Pb$	$^{208}UPb/^{232}Th$ age (Ma)	$^{206}Pb/^{238}U$ age (Ma)
2.1	1	2	2969	140	1.15	57.4	0.0571 ± 23	435.9 ± 17	21 ± 11	14.6 ± 0.6
4.1	1	2	2698	649	1.83	35.4	0.0634 ± 28	412.1 ± 16.2	17.1 ± 5.3	15.3 ± 0.6
5.1	1	1	450	250	9.21	57	0.132 ± 166	406.9 ± 23.5	15 ± 7.7	14.4 ± 0.8
6.1*	1	1	211	77	20.47	66.1	0.2379 ± 94	60.9 ± 2.8	204 ± 66	83.7 ± 3.8
6.2	1	2	882	149	10.91	74.2	0.1479 ± 82	397.3 ± 19.8	27.8 ± 14	14.4 ± 0.7
7.1	1	1	1566	78	2.11	83.6	0.0659 ± 28	398.4 ± 15.7	9.9 ± 8.5	15.8 ± 0.6
8.1	1	1	689	47	3.83	509.9	0.0951 ± 21	9.9 ± 0.4	0 ± 0	599 ± 23
8.2	1	2	2560	760	1.61	28.2	0.0613 ± 19	411.8 ± 16	14.8 ± 3.9	15.4 ± 0.6
9.1	2	1	168	95	0.53	6.2	0.0681 ± 16	8.5 ± 0.1	739 ± 22	717 ± 8.7
10.1	2	1	205	103	0.27	3.9	0.0755 ± 9	5.8 ± 0.1	986 ± 22	1016 ± 9.2
11.1	2	1	239	334	4.49	19.5	0.0881 ± 94	411.9 ± 24.3	14.6 ± 1.3	14.9 ± 0.9
12.1	2	1	312	109	3.48	37.8	0.0787 ± 64	533.8 ± 30.3	14 ± 2.2	11.6 ± 0.7
13.1	2	1	236	104	0	0	0.091 ± 24	4 ± 0.1	1515 ± 106	1437 ± 33
14.1	2	1	138	137	0.16	1.2	0.0655 ± 13	8.2 ± 0.1	738 ± 12	743 ± 6.2
15.1	2	1	542	129	1.15	30.6	0.0575 ± 24	155.8 ± 2.3	31.8 ± 3.7	40.8 ± 0.6

Session date: 1 27/05/96
2 18/06/96
*Spot 6.1 results affected by inclusion.

Table 3. *Ar–Ar age spectrum data for sample 95–481 hornblende (Tinit batholith)*

Temp (°C)	^{36}Ar (mol)	^{37}Ar (mol)	^{39}Ar (mol)	^{40}Ar (mol)	% radiog.	$^{*40}Ar/^{39}K$	Cumulative release	Age (Ma)	Error	Ca/K
700	6.32E-16	5.83E-16	1.38E-16	1.94E-13	3.6	50.61	0.63	70.26	45.52	8.08
900	2.26E-16	3.67E-15	4.12E-16	8.30E-14	20.0	40.44	2.51	56.36	3.18	17.00
1000	1.06E-16	2.31E-15	4.88E-16	5.06E-14	38.4	39.96	4.74	55.70	1.56	9.03
1060	1.38E-16	9.34E-15	6.91E-16	7.49E-14	46.7	50.97	7.88	70.75	1.93	25.90
1100	2.51E-16	2.66E-14	1.94E-15	1.80E-13	60.4	56.40	16.72	78.12	0.60	26.20
1140	3.22E-16	5.20E-14	5.02E-15	3.50E-13	74.3	52.05	39.61	72.22	0.24	19.80
1160	1.80E-16	2.42E-14	2.50E-15	1.81E-13	71.9	52.12	51.03	72.32	0.55	18.50
1170	1.23E-16	1.35E-14	1.38E-15	1.07E-13	67.2	52.43	57.30	72.73	0.63	18.70
1190	1.21E-16	1.36E-14	1.41E-15	1.07E-13	67.8	51.63	63.72	71.64	0.71	18.40
1220	1.37E-16	2.29E-14	2.23E-15	1.55E-13	75.5	52.87	73.88	73.34	0.34	19.60
1240	1.08E-16	1.24E-14	1.14E-15	9.37E-14	67.2	55.84	79.05	77.37	0.67	20.90
1265	1.27E-16	1.23E-14	1.14E-15	1.00E-13	63.8	56.28	84.25	77.96	0.88	20.60
1290	1.40E-16	1.34E-14	1.28E-15	1.12E-13	64.1	56.25	90.10	77.92	0.60	20.00
1330	1.71E-16	1.16E-14	1.08E-15	1.10E-13	55.1	56.42	95.03	78.15	0.98	20.50
1450	4.55E-16	1.32E-14	1.09E-15	1.94E-13	31.3	56.09	100.00	77.70	2.57	23.10
Total	3.24E-15	2.32E-13	2.19E-14	2.09E-12	53.07		73.6 ± 1.02			

Lambda K40 = 5.54E-10 J = 7.85E-04

Table 4. *Ar–Ar age spectrum data for sample 95–411 K-feldspar (Ladakh batholith)*

Temp (°C)	^{36}Ar (mol)	^{37}Ar (mol)	^{39}Ar (mol)	^{40}Ar (mol)	% radiog.	$^{*40}Ar/^{39}K$	Cumulative release	Age (Ma)	Error	Ca/K
450	2.87E-16	1.13E-16	4.18E-16	1.25E-13	32.3	96.738	0.16	264.24	9.63	0.513
450	8.58E-17	8.32E-16	2.26E-16	2.72E-14	7.1	8.598	0.25	25.12	4.02	7.030
500	1.07E-16	2.74E-16	6.80E-16	8.46E-14	62.5	77.692	0.52	215.18	2.65	0.765
500	3.84E-17	5.96E-17	5.11E-16	1.48E-14	23.0	6.628	0.72	19.39	1.13	0.222
550	1.40E-16	7.23E-16	2.16E-15	1.54E-13	73.2	52.296	1.58	147.63	0.5	0.636
550	2.94E-17	6.68E-17	1.32E-15	1.68E-14	48.1	6.112	2.1	17.89	0.35	0.096
600	9.26E-17	1.99E-16	2.62E-15	9.88E-14	72.3	27.284	3.13	78.53	0.53	0.144
600	2.04E-17	6.69E-17	1.52E-15	1.53E-14	60.5	6.104	3.73	17.87	0.21	0.084
650	6.35E-17	6.70E-17	2.43E-15	6.63E-14	71.6	19.594	4.69	56.74	0.3	0.052
650	1.63E-17	6.70E-17	1.55E-15	1.50E-14	67.7	6.541	5.3	19.14	0.22	0.082
700	4.69E-17	6.71E-17	2.22E-15	4.59E-14	69.7	14.411	6.18	41.9	0.23	0.057
700	9.37E-18	6.71E-17	1.66E-15	1.34E-14	79.1	6.351	6.84	18.59	0.22	0.077
750	2.28E-17	7.92E-16	1.89E-15	2.41E-14	72.1	9.185	7.58	26.82	0.35	0.796
750	6.72E-18	6.72E-17	1.80E-15	1.33E-14	84.8	6.256	8.3	18.31	0.15	0.071
800	1.38E-17	1.03E-16	1.75E-15	1.61E-14	74.6	6.892	8.99	20.16	0.31	0.112
800	7.48E-18	1.49E-15	1.94E-15	1.40E-14	85.1	6.147	9.75	17.99	0.21	1.460
850	1.79E-17	6.74E-17	1.74E-15	1.70E-14	68.6	6.702	10.44	19.61	0.21	0.074
850	1.25E-17	9.28E-16	2.00E-15	1.60E-14	77.3	6.220	11.23	18.2	0.18	0.884
900	3.60E-17	8.39E-18	1.80E-15	2.32E-14	54.0	6.979	11.94	20.41	0.27	0.009
900	2.82E-17	2.80E-16	2.10E-15	2.32E-14	64.0	7.060	12.76	20.65	0.23	0.253
950	7.03E-17	6.76E-17	2.18E-15	3.84E-14	45.8	8.063	13.63	23.56	0.42	0.059
950	6.88E-17	7.65E-16	2.94E-15	4.57E-14	55.5	8.613	14.79	25.16	0.31	0.494
950	1.16E-16	1.18E-16	4.38E-15	7.73E-14	55.4	9.782	16.52	28.55	0.26	0.051
1000	1.21E-16	9.46E-16	3.50E-15	7.62E-14	53.3	11.609	17.9	33.83	0.18	0.513
1000	1.19E-16	7.07E-17	5.30E-15	9.45E-14	62.8	11.185	20	32.6	0.16	0.025
1050	1.76E-16	3.79E-17	7.47E-15	1.44E-13	63.9	12.344	22.95	35.95	0.19	0.010
1050	1.59E-16	1.61E-15	1.01E-14	1.69E-13	72.1	12.010	26.94	34.99	0.14	0.301
1050	1.80E-16	3.61E-15	1.36E-14	2.20E-13	75.9	12.329	32.3	35.91	0.22	0.506
1100	1.25E-16	2.08E-15	8.15E-15	1.49E-13	75.1	13.691	35.52	39.83	0.34	0.484
1100	1.17E-16	2.49E-16	1.05E-14	1.73E-13	80.0	13.181	39.67	38.36	0.11	0.045
1100	1.34E-16	1.56E-15	1.41E-14	2.31E-13	82.8	13.530	45.24	39.37	0.13	0.210
1100	1.51E-16	2.06E-15	1.60E-14	2.66E-13	83.2	13.798	51.57	40.14	0.11	0.244
1100	1.56E-16	1.45E-15	1.59E-14	2.71E-13	83.0	14.138	57.85	41.12	0.13	0.173
1100	1.78E-16	1.29E-15	1.63E-14	2.86E-13	81.5	14.304	64.3	41.59	0.13	0.150
1100	1.91E-16	3.43E-15	1.52E-14	2.77E-13	79.7	14.480	70.32	42.1	0.16	0.428
1100	2.81E-16	2.68E-15	1.85E-14	3.51E-13	76.3	14.493	77.62	42.14	0.15	0.275
1200	1.12E-16	1.24E-16	1.16E-14	1.99E-13	83.1	14.198	82.21	41.29	0.11	0.020
1230	1.63E-16	1.24E-16	1.69E-14	2.86E-13	83.1	14.048	88.89	40.86	0.11	0.014
1260	1.51E-16	1.24E-16	1.52E-14	2.56E-13	82.5	13.906	94.88	40.45	0.12	0.016
1290	9.75E-17	2.15E-15	8.54E-15	1.45E-13	80.1	13.579	98.25	39.51	0.22	0.479
1320	4.92E-17	1.82E-15	3.05E-15	5.59E-14	74.2	13.612	99.45	39.61	0.28	1.140
1350	2.80E-17	1.24E-16	8.93E-16	1.99E-14	58.3	12.957	99.81	37.72	1.06	0.265
1450	4.07E-17	2.05E-16	4.88E-16	1.84E-14	34.6	13.052	100	37.99	1.91	0.800
Total	4.07E-15	3.30E-14	2.53E-13	4.67E-12	13.7	39.86 ± 0.21 Ma				
Lambda K40 = 5.54E-10 J = 1.63E-03										

whereas all other data points required less than 2%) and very different $^{206}Pb/^{238}U$, $^{207}Pb/^{235}U$ and $^{208}Pb/^{206}Pb$ ages. The youngest age in the remaining group (11a) required a relatively high common lead correction and the spot that yielded the oldest point (99a) has overlapped with a small inclusion, and these analyses may not have yielded the correct crystallization age of the zircons.

Hornblende diorite 95–481 is composed mainly of plagioclase and hornblende. There are books of chlorite adjacent to concentrations of hornblende, but the amphiboles themselves are fresh looking and do not contain visible chlorite. A pure separate of the hornblende was obtained by conventional separation methods and a $^{40}Ar/^{39}Ar$ step heating analysis was undertaken on a several milligram aliquot. The results (Table 3) are presented as an age spectrum diagram in Fig. 6. The age spectrum is relatively flat for the majority of gas release, such that a plateau age calculated for the middle portion of

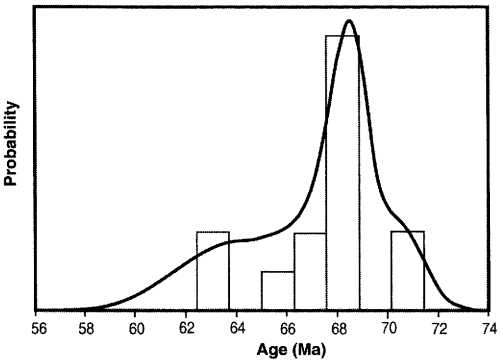

Fig. 5. Histogram of $^{238}U/^{206}Pb$ ages obtained from ion-microprobe analyses of zircons from a Tirit tonalite (sample 96–711; Table 1; location in Fig. 1b). The smooth curve indicates the relative probability plot of the data, constructed by assigning an equal-area Gaussian distribution to each analysis and assuming these over the entire age range.

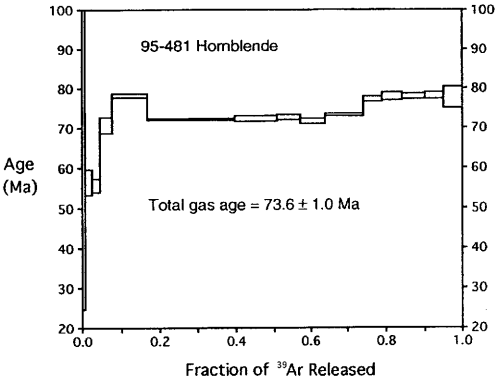

Fig. 6. Age spectrum diagram for hornblende 95–481.

gas release would not be very different from the integrated total gas age of 73.6 ± 1.0 Ma (1σ). A K/Ca for over 90% of gas release is below about 0.06, which indicates no significant contamination of the separate. An isochron plot of all of the data points is in agreement with the age spectrum results, yielding an age of 73.1 ± 1.1 Ma (1σ with MSWD), and the data do not show any clear evidence for excess argon contamination. Thus, we prefer the age of 73.6 ± 1.0 Ma, which we interpret as being very close to the age of crystallization of the diorite, similar to the U–Pb zircon crystallization age determined for the granite at Tirit. This limited dataset suggests that the Tirit batholith intrusion is between 74 Ma to 68 Ma.

Karakoram leucogranite—U–Pb

We carried out U–Pb SHRIMP dating of zircons from a typical leucogranite sample collected north of Satti (sample 021, location in Fig. 1b). Cathodeluminescence images of the zircons revealed idiomorphic zircons with cores truncated by the later growth of rims with fine zonation (Fig. 7a). The position of spots for analysis were chosen according to internal zoning of zircons as revealed by cathodeluminescence. Dating methodology was described in Weinberg & Dunlap (in press). The SHRIMP II at the Australian National University was used and the primary ion beam was focused to spots approximately 30 μm in diameter. The standard used was SL13 (Claoué-Long *et al.* 1995) and two standards were analysed for every four analyses of unknown zircons. Results were corrected for common lead by assuming the isotopic composition of lead from Broken Hill, Australia (the composition of Pb impurities found in exhaust fans at the ANU laboratory). For each analysis, seven cycles were carried out, each cycle measuring the secondary ion yields of Zr_2O^+, the four lead isotopes (^{208}Pb, ^{207}Pb, ^{206}Pb, ^{204}Pb), U^+ and UO^+, Th^+ and ThO^+. Because neither $^{207}Pb/^{206}Pb$ nor $^{207}Pb/^{235}U$ chronology by SHRIMP provide a fine age resolution for the Phanerozoic, we relied entirely on the $^{206}Pb/^{238}U$ and $^{208}Pb/^{232}Th$ geochronometers.

Seven analyses of well-developed zircon rims defined a single young group centred at 15.0 ± 0.4 Ma (2σ) which we interpret as the age of crystallization of the granite (Table 2 and Fig. 7b). One spot was excluded because it yielded a much younger age (11 Ma spot number 12.1) which we considered to be an outlier. Zircon cores yielded a wide spread in ages indicating zircon inheritance. The two U–Pb zircon age determinations for the eastern Karakoram leucogranites now available (15.0 ± 0.4 Ma and 18 ± 0.6 Ma; here and Searle *et al.* 1998, respectively) suggest leucogranites east of the KF are younger than those to the west (20–25 Ma; Parrish & Tirrul 1989; Schärer *et al.* 1990; Fig. 2b).

Thermal history of the Ladakh granite adjacent to the KT

In this section we present thermal modelling, effectively an interpretation, of the results of $^{40}Ar/^{39}Ar$ step heating of a K-feldspar concentrate from Ladakh granite 95–411, which intruded the base of the Shyok Fm. near the bridge at Hundar (Table 4). It is clear from recent U–Pb ion microprobe work that the bulk of the Ladakh batholith crystallized about 60 Ma

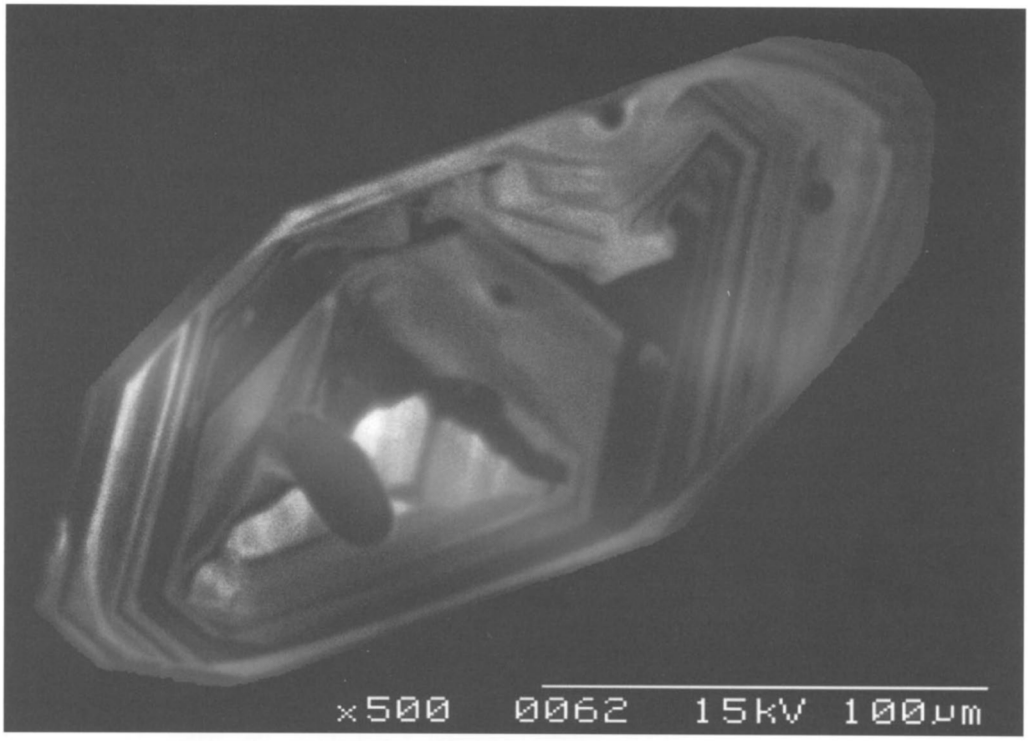

(a)

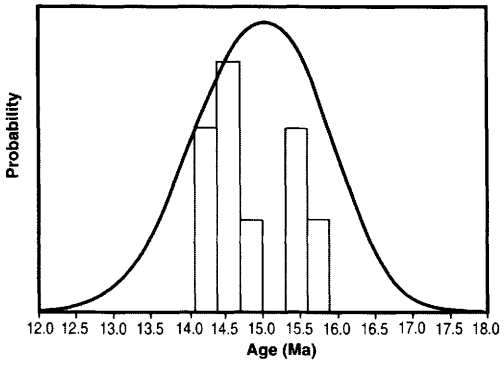

(b)

Fig. 7. (**a**) Cathodeluminescence image of a zircon from sample 021 from N of Satti (Karakoram leucogranite see Fig. 1 for location). (**b**) Histogram of $^{238}U/^{206}Pb$ ages obtained from ion-microprobe analyses of zircons from sample 021; Table 2. The smooth curve indicates the relative probability plot of the data, constructed by assigning an equal-area Gaussian distribution to each analysis and assuming these over the entire age range.

(Weinberg & Dunlap in press), and we use this information as a control point for the thermal modelling.

We assume that the degassing of argon from the sample in the laboratory and that the closure to argon loss during natural cooling is governed by Fickian diffusion, and that the process is effectively reversible. The modelling provides a non-unique continuous cooling path, discussed below. Although non-unique, it will be seen from the solution that the true thermal path experienced by the sample must fall within narrow limits if the assumption of Fickian diffusion is valid. We interpret the results in terms of cooling through a closure temperature range of about 350–150 °C, the typical closure temperature window accessed by K-feldspar (e.g. Lovera *et al.* 1997). The justification for this procedure, outlined in detail by Lovera *et al.* (1997), is that K-feldspars commonly contain pronounced age gradients which cannot be produced by diffusive loss of argon from a single domain. The analytical procedures were essentially the same as those cited by Weinberg

& Dunlap (in press). The step heating results for 95–411 K-feldspar have been inverted into a time–temperature history following the method of Lovera *et al.* (1989). A multi-diffusion domain solution comprising eight domains, all with activation energies of 54.0 kcal mol^{-1}, has been calculated using the time, temperature and fraction of ^{39}Ar released during the course of the degassing experiment. Using this distribution of model diffusion length scales, and the volume fractions of each length scale, thermal paths were calculated by inputting trial thermal histories and minimizing the differences between the measured and modelled age spectra by manual iteration.

The age spectrum derived from detailed step heating of 95–411 K-feldspar, shown in Fig. 8, shows that the sample was not able to finally close to loss of argon until about 18 Ma. Subsequent to cooling from magmatic temperatures at 60 Ma the sample must have cooled to below *c.* 310 °C by about 40 Ma, indicating a cooling rate of at least 20–30 °C Ma^{-1}. Without this initial rapid cooling good model fits are not possible. For a monotonically declining temperature history, one where there is never reheating between the time of intrusion and about 18 Ma, the sample could have experienced 310 °C as a maximum sustainable temperature for this entire period (thermal history shown in Fig. 8). Significant excursions in temperature from the curve shown in Fig. 8b are permissible. However, for temperature spikes with a duration of *c.* 5 Ma a peak temperature of no more than *c.* 340 °C can be sustained and still allow good model fits. From these simple model calculations it is clear that the sample never experienced temperatures greater than greenschist facies conditions (*c.* 250–450 °C) subsequent to cooling rapidly from magmatic temperatures. Age resolution is lost at 18 Ma, but the subsequent thermal history still has an effect of the model age spectrum. To obtain good model fits we have maintained model temperatures in the greenschist facies range until well after 18 Ma.

It is consistent with our geological observations that these rocks experienced greenschist facies temperatures for long periods. Although alternative models involving reheating are equally as likely to have been responsible for the age gradient preserved in K-feldspar 95–411, reheating for any significant time span (> 5 Ma) is limited to temperatures not exceeding *c.* 340 °C. The contact relationships between the Shyok Fm. and the Ladakh granites suggest that the granites were intruded into a volcano-sedimentary section that was already folded. Regardless of the exact form of the postmagmatic thermal history, it is clear that after cooling to below about 310 °C shortly after intrusion, greenschist facies temperatures were maintained for an extended period between 60 and 18 Ma, and perhaps throughout this whole time span. These results suggest that the greenschist facies assemblages preserved in rocks deformed by the KT, cropping out one or two kilometres to the north, are indicative of the conditions prevailing during most of the deformation.

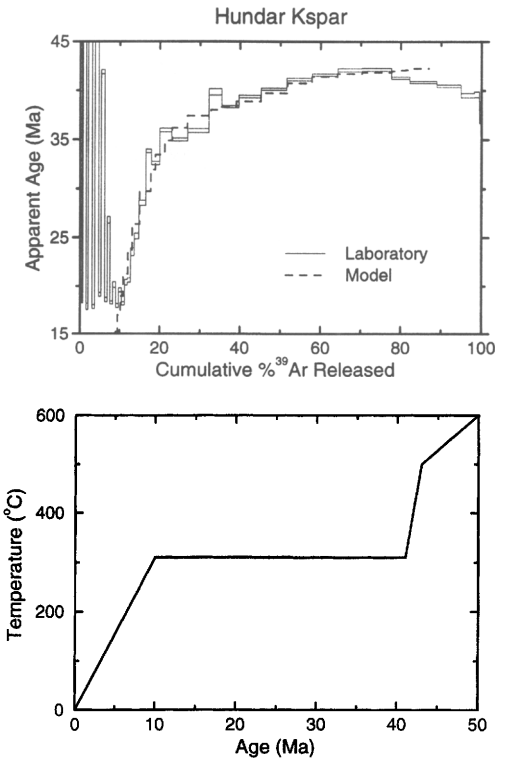

Fig. 8. Age spectrum and thermal history diagrams for K-feldspar sample 95–411. (**a**) Laboratory derived and model age spectra. Note the close fit of the model age spectrum to the laboratory result. (**b**) Thermal history used as input to the modelling program. The calculated domain distribution is combined with the thermal history to produce the theoretical age spectrum model in (a).

Structural analysis

In this section we analyse the structures measured on the Khalsar Thrust (KT) and Karakoram Fault (KF) and derive their possible kinematic relationship. The N60W-striking KT merge with the N30W-striking KF immediately east of the confluence. East of this point the main

strike of the KF changes to N40–45W (Fig. 1b insert) and lineation steepens. We divide the study of the faults into three parts: the KT, the KF west of the confluence (KF–Nubra) and the KF east of the confluence (KF–Shyok). Because the KF–Shyok close to the confluence is mostly covered by Quaternary sediments of the Shyok River, our study of this part concentrates on the area between the Shyok, Darbuk and Tangtse (Fig. 1a), 60 km east of the confluence.

Mineral lineation (chlorite, epidote and quartz) on the KT is generally steep but somewhat shallower than down dip (Fig. 9a), indicating a small dextral component. Thrusting, as observed near Khalsar (Fig. 3), is confirmed by S–C fabric in the greenschists and lineation plunge. A cataclastic rock closest to the thrust contact suggests brittle reactivation. The KT strikes N55–60W/55–60 NE, roughly parallel to penetrative foliation. An outcrop marking the northern limit of the fault zone is characterized by an epidote-rich rock (hydrothermal alteration), where S–C fabric (C = N45W/45SW and S = N45W/65SW) indicates south-side up-thrust, parallel to down-dip lineation (Fig. 10). The geometry and sense of shear determined at the north and south margins of the KT (Fig. 10) suggest a flower structure, where rocks within the shear zone have been squeezed upwards.

The N30W KF–Nubra has displaced regional markers dextrally (e.g. Searle *et al.* 1998). Most foliations within the fault zone strike between N30W and N50W, in accordance with dextral shearing. The dip of the foliation within the Nubra Fm. gradually steepens towards the contact with the Karakoram leucogranite, where it is nearly vertical (shown schematically in Fig. 2a). Mineral and stretching lineations as well as crenulation axis are generally 10° from the horizontal (Fig. 9b), and kinematic indicators confirm dextral shearing. The sheared plutonic rocks at Kubed define the Kubed Shear Zone, within which strain varies considerably, and form a band 200–300 m wide of mylonites and where foliation is generally subvertical striking N40–60W. We interpret the Kubed Shear Zone as a splay of the main KF.

The KF–Shyok's main strike is intermediate between that of the KF–Nubra and the KT, at N45W (Fig. 9c). Near Darbuk and Tangtse the shear zone is up to 10 km wide and represents a sharp boundary between rocks of the Ladakh block (Khardung Fm. and Ladakh granitoids) from rocks of the Karakoram terrane. Foliation generally strikes N40–50W but dips vary from 70 SW to subvertical near Shyok village, on the northern part of the shear zone, to 60–70 NE at Tangtse, on the southern edge of the zone (Fig. 9c). Lineation plunges between 50° N and 25° N (more commonly 40–45° N), and over 30 observations of kinematic indicators in the Darbuk and Tangtse gorges, suggest dextral north-side-up sense of shear (including the mylonites limiting the shear zone north and south). Brittle faults in the Darbuk Gorge suggest similar kinematics during brittle deformation. Thus, the KF–Shyok combines elements of both the KT and the KF–Nubra, striking at an intermediate angle and combining roughly equal components of thrusting and dextral strike-slip movement.

Vector analysis

Oblique dextral movement on the KF–Shyok may be interpreted as being partitioned, west of the confluence, into thrusting on the KT and dextral strike-slip on the KF-Nubra (Fig. 9). Whereas the two sections of the KF seem to be kinematically linked and presently active, we have no evidence on the timing of motion on the KT. Thus the KT could either be (a) older and unrelated to the KF, or (b) contemporaneous and kinematically linked to the KF. In order to test whether the faults may all be kinematically linked, we carried out vector analysis of the relative horizontal motion between the three blocks (Fig. 11). We assume that the measured lineations are true measures of the relative motion of blocks at the triple junction, and assume no relative rotation of blocks. At the outset we note that the data for the KF–Shyok define a range of possible horizontal movement directions between the Ladakh (LAD) and Karakoram (KAK) blocks varying from N20W to N60W (Fig. 11b), suggesting internal deformation of the shear zone. Similarly, lineation plunges on the KT (Fig. 9) define a range of possible movement directions, most likely between N30E (down dip) and N15E (thrust with a small dextral component).

For the case of an older KT, relative movement between LAD and the Saltoro Block (SAL) is zero during slip on the KF. In this case the N30W strike-slip motion on the KF–Nubra is maintained along the KF–Shyok and the movement vector SAL–KAK is equal to LAD–KAK (Fig. 11c). Vector analysis indicates that contemporaneous movement on the KT and KF is consistent with the structural data and allows further constraints of their relative motion (we stress, however, that consistency is not proof of their contemporaneity). Structural data from the KT define a NNE-trending vector of undefined length between LAD–SAL. This vector direction constrains the broad range of

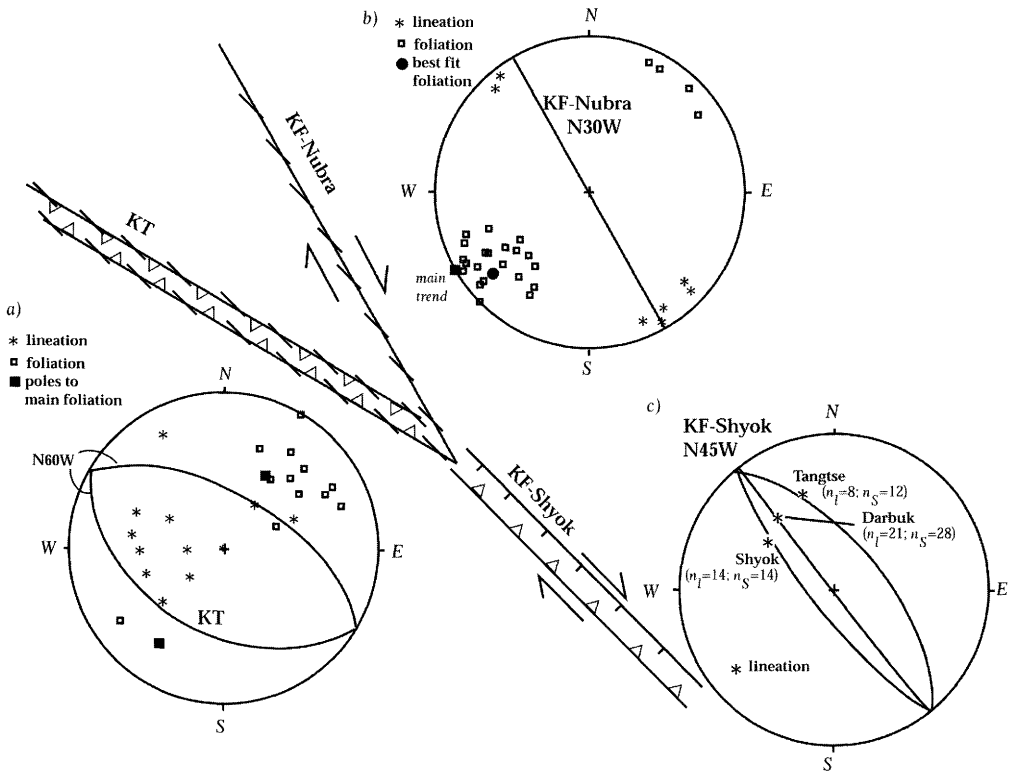

Fig. 9. Summary of the main structural observations in the Nubra–Shyok confluence and lower hemisphere, equal-area stereonet projections of the structural data collected in the three different structural domains. (**a**) Khalsar Thrust between the villages of Khalsar and Deshkit. Poles to foliation tend to plot along a small clockwise angle from the main trend of the thrust zone (solid black square is the pole to one of the two great circles indicating main trend of the KT). Lineation tends to plunge slightly NW of down dip, suggesting a small dextral component on this fault. In (a) lineation plunges close to down dip predominate over shallower plunges, although this is not clear in the figure, because each of these down-dip plunges represents the typical value of long outcrop surfaces, whereas each of the shallower plunges are more anomalous, single measures. (**b**) KF–Nubra between Panamik and Sumur–Tirit. Poles to foliation tend to plot at a small anticlockwise angle from the main trend of the fault zone marked by the great circle. The strike of the foliation in both the KT and KF–Nubra are nearly parallel to each other (*c.* N45W) and are parallel to the main trend of the KF–Shyok (marked in the figure). Each measurement in (b) is the typical value for individual outcrops. (**c**) KF–Shyok between the villages of Shyok–Darbuk–Tangtse and along the Tangtse Gorge (see inset on Fig. 1b for location). This area was divided into three geographical domains, corresponding to the northern margin of the shear zone (Shyok), the core of the zone (Darbuk), and to a 2 km wide band on the southern margin of the zone (Tangtse), and the mean lineation and foliation for each area are plotted. Lineation plunges *c.* 40–45° NNW, and the strike of the foliation is nearly constant at N40W but dips vary systematically from steep SW at the north to moderate NE at the south. Kinematic indicators in all three areas define a dextral, north-side-up movement. Each great circle or lineation is the average value for the data collected in each particular subdivision.

possible movement direction between LAD–KAK to values between N30W and N20W. For increasingly important horizontal movement rates across the KT (longer LAD–SAL vector), the more the relative motion between LAD–KAK is forced towards N20W (more northerly directions are inconsistent with lineation directions in KF–Shyok). These relations allow prediction of the relative motions between the three blocks (Fig. 11c), which may be tested by determining present-day horizontal movement rates across two out of the three faults.

Discussion

Nubra Fm. and Karakoram Fault

Nubra Fm. rocks have been dated as Permian by Thakur *et al.* (1981) and Thakur & Misra (1984), based on fossil fauna recovered from limestones.

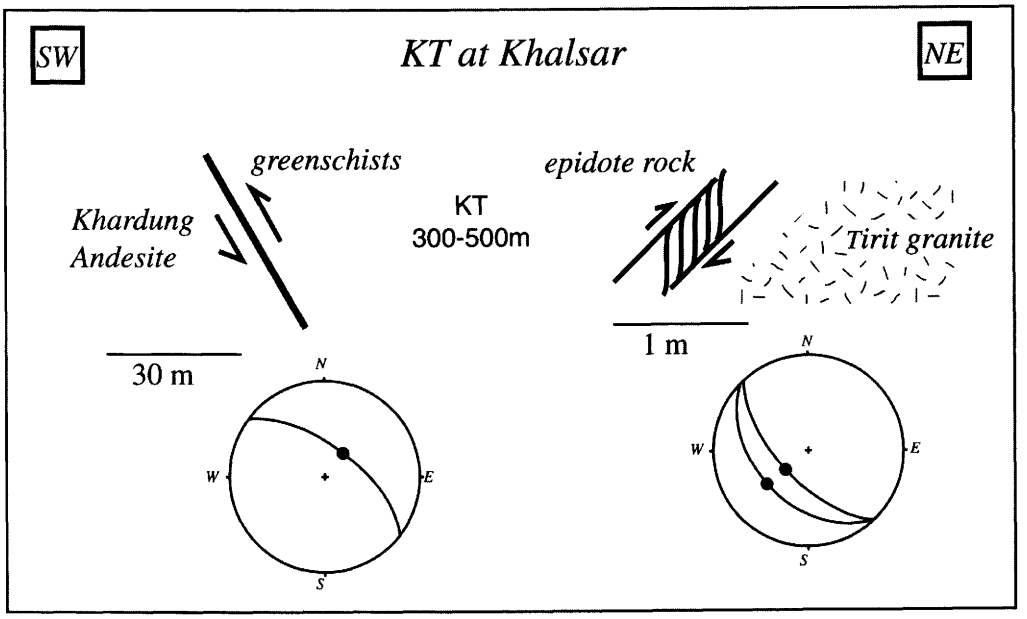

Fig. 10. Schematic summary of the observations defining the flower structure near Khalsar. Contact between the northern margin of the shear zone and Tirit batholith was not observed, but those granitoids crop out tens of metres north of the epidote-rich fault rock.

Rocks of Permian age have also been found within the Shyok Suture Zone (Pudsey 1986) and north of the MKT in Pakistan (Gaetani *et al.* 1990). We have found only minor occurrences of fully recrystallized limestone, which would have lost any evidence of fossils. The Nubra Fm. represents a (disrupted?) volcano-sedimentary sequence intruded by Karakoram leucogranites, neither of which have been found south of the KF. The lack of ultramafic rocks and chert argue against it being a disrupted ophiolite sequence. The intrusive contacts between the Karakoram leucogranite and Nubra Fm., and the apparent absence of Karakoram leucogranites in the northern Saltoro Range, suggest that the Nubra Fm. belongs to the Karakoram terrane and that this terrane was tectonically placed in contact with rocks of the Saltoro Range, which record a different geological history. If this interpretation is correct, there must be another fault, possibly brittle, between the Nubra Fm. and the Tirit batholith to the west. In Searle *et al.* (1998), we used the lack of Karakoram granites south of the KF to argue that faulting should have started after intrusion of the 18 Ma leucogranite (age of the Karakoram leucogranite at Tangtse). The 15 Ma age of the Satti (Karakoram) leucogranite suggests an even later initiation of the KF.

KF–Shyok—sense of shear

In Searle *et al.* (1998), we have suggested that the high-grade rocks of the Pangong Range represent deeper crustal rocks exhumed through transpression between the two strands of the KF at Tangtse. These high-grade rocks are in tectonic contact with medium-grade limestone and shales (with staurolite and garnet), to the north of the fault, and weakly metamorphosed rocks of the Ladakh block to the south. The north-side-up and dextral sense of movement determined here throughout the width of the KF–Shyok is similar to that interpreted from one fault escarpment, caused by Quaternary earthquake on the north (Pangong) strand of the KF (Brown & Molnar pers. comm.). These observations imply that rocks north of the fault should be deeper and hotter than those within the KF–Shyok and not medium-grade rocks. This contradiction needs to be further investigated. A more complex faulting history is suggested by de Terra's (1932) observation that the medium-grade rocks north of the KF–Shyok form only a narrow band, followed northwards by high-grade rocks intruded by Karakoram leucogranites.

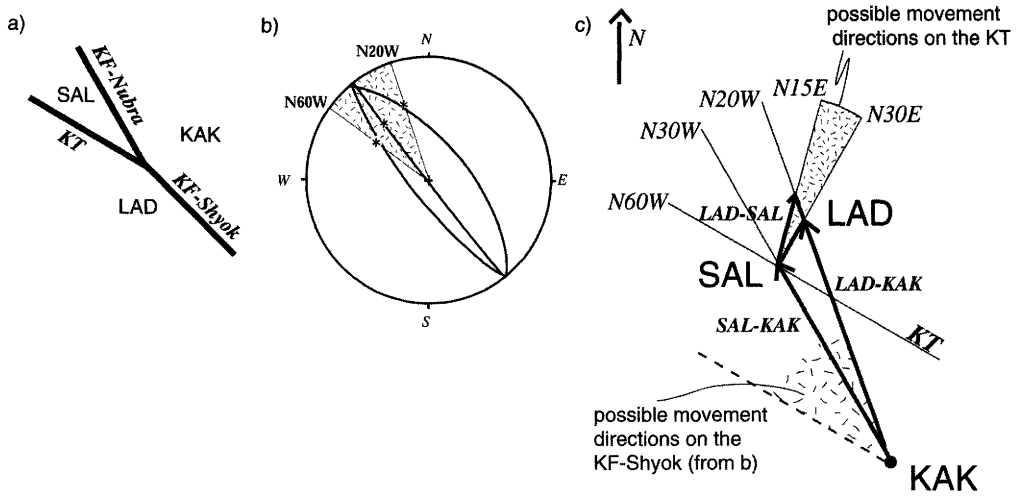

Fig. 11. (**a**) Three blocks and triple point defined by the intersection between the KT, KF–Nubra and KF–Shyok. (**b**) Horizontal projection of the average lineation of the three structural domains of the KF–Shyok, constraining the possible range of horizontal movement direction between LAD and KAK to between N20W and N60W (dashed region; also indicated in c). (**c**) Vector analysis of the triple junction. The dimensions of the vectors between the blocks are unknown, thus the analysis can only yield vector orientation and relative length of these vectors assuming the KAK–SAL vector is unity. For inactive KT during KF slip, the vector LAD–SAL is zero, and the horizontal displacement rate between LAD–KAK is equal to that between the SAL–KAK. For an active KT, LAD–SAL vector trends between N15E and N30E (as constrained by lineation; stippled area) and constrains the movement vector direction LAD–KAK to N30W–N20W. The two small arrows between SAL and LAD indicate a range of possible LAD–SAL vector lengths, from zero (KT inactive), to a maximum length of 0.22 to 0.31 (depending on whether we take the N30E or N15E orientation limits, respectively). The vector LAD–KAK varies from being unity (equal to the SAL–KAK vector, no thrusting on the KT) to a maximum of 1.24 (24% faster than SAL–KAK).

Suture zone and terrane boundary

Although all suture zones are terrane boundaries, not all terrane boundaries are suture zones. Northern Ladakh is an excellent example of this difference. A suture zone defines the region where two continents collided. Suture zones are generally characterized by the presence of heavily sheared and tectonically disaggregated marine sediments and oceanic crust separating terranes of entirely different histories. However, what defines a suture zone is not the presence of marine/oceanic rocks, but the fact that it represents the actual collision site. Thus, whereas the SSZ described in Baltistan represents a suture zone, the sharp terrane boundary between the Ladakh and Karakoram blocks across the KF–Shyok is not the site of suturing, but a boundary caused by post-suturing strike-slip.

Several authors suggested the presence of the Shyok Suture Zone near the confluence area. We were unable to find such rocks. Neither the Nubra Fm. nor the Shyok Fm. and its sheared equivalents within the KT define the suture zone. This suggests that the SSZ runs north of the KT. Srimal (1986*a*, *b*) described the Biagdang ophiolite immediately north of the KT, on the southern slopes of the Saltoro Range. This ophiolite is an obvious candidate for the suture zone, but although we have not been able to reach that area, we are not entirely satisfied that the rocks he described are from an ophiolite. This is partly because Srimal, and most other workers that described these rocks, have presented little data to support their interpretations, partly because authors very often contradict one another, and partly because our few observations on the Saltoro Range contradict Srimal's observations. For example, the map of Rai (1982) shows flysch and molasse where Srimal (1986*a*, *b*) mapped the ophiolite. In Kubed on the northeastern slopes of the Saltoro, where Srimal described the Saltoro ophiolite, we found a sequence of sheared granitoids, diorites and gabbros and cumulitic pyroxenite, all apparently related to Tirit magmatism and not to an ophiolitic sequence.

Descriptions of the geology of the Saltoro Range suggest that its post-75 Ma evolution is similar to that of the northern Ladakh Range. Within the Saltoro Range, Rai (1982) describes a reddish-brown volcanic rock forming dykes and volcanic layers, characterized by random

distribution of euhedral plagioclase phenocrysts in fine ground mass, similar to our Khardung Andesite Unit. Furthermore, Srimal (1986*a*, p. I–10) describes rocks similar to the Khardung Fm. on the Saltoro Range, as well as granitoids (Tirit?) intruding the basic–ultrabasic sequence of the south Saltoro Range. More importantly, the 68 ± 1 Ma crystallization age of our Tirit sample coincides with the age range of Ladakh granitoids, and field relations suggest that the Ladakh and Tirit batholiths may be part of the same magmatic event. We conclude that, if the basic–ultrabasic rocks of the Saltoro Range represent a suture zone, suturing must have occurred before *c.* 75 Ma, confirming conclusions from Baltistan and Kohistan (collision estimates ranging between 85 and 100 Ma, e.g. Petterson & Windley 1985, 1992; Pudsey 1986; Hanson 1989; Treloar *et al.* 1989, 1996; Brookfield & Reynolds 1981). In fact, similar granitoid ages have also been found in the Karakoram Range in Pakistan (Rb–Sr isochron age of 63 ± 2 Ma, Debon 1995) and inferred from igneous zircon core ages from the Tangtse leucogranite (cores of 63.0 ± 0.8 Ma (2σ), Fig. 2b and Searle *et al.* 1998). The geology of the Ladakh and Saltoro blocks is in stark contrast to the geology of the Karakoram terrane. The absence of the 18–15 Ma Karakoram leucogranites, south of the KF, suggests that the Karakoram block was far removed from the Ladakh–Saltoro blocks during leucogranite intrusion.

Regional correlations

The MKT was originally defined in Pakistan as the late Tertiary fault that places Karakoram metamorphic rocks (Eurasian rocks) south over the SSZ or Ladakh–Kohistan batholiths (Dras–Kohistan arcs). In Ladakh most previous authors have referred to the Khalsar Thrust as the MKT. However, there is at present insufficient evidence to enable correlation between the KT and the MKT in Baltistan. Neither its age nor the geology of the two blocks across the fault are sufficiently well-known to be able to establish the correlation. From our observations and literature survey, we concluded that at least the post-75 Ma geology of the Ladakh and Saltoro blocks are the same. Furthermore, we found no evidence that could support the presence of ophiolites in the southern Saltoro.

The rock sequence described above may be correlated to those of Baltistan and Kohistan. The Cretaceous Shyok Fm. corresponds to the tholeiitic, Cretaceous Chalt volcanic group (Treloar *et al.* 1996; also named the Hunza Valley volcanic group by Petterson *et al.* 1990) which crops out south of the MKT in Pakistan. The Ladakh batholith is part of the long calc-alkaline igneous belt that to the west is represented by the Kohistan batholith of similar age and composition (Petterson & Windley 1985, 1991). The Khardung Fm, extruded on top of the Ladakh batholith, corresponds in age and composition to the Eocene Dir–Utror Gp of Kohistan (e.g. Tahirkheli *et al.* 1979; Petterson & Windley 1985, 1991; Sullivan *et al.* 1993). The SSZ lies immediately north of the MKT in Kohistan and Baltistan and most likely follows east towards the KF and crops out somewhere within the Saltoro Range. The less competent volcanic and sedimentary rocks lying in between the Ladakh and Karakoram batholiths were intensely deformed and disrupted by the KF. At the confluence the two batholiths are separated only by the narrow strip of sheared rocks of the Nubra Fm., as opposed to a *c.* 30 km wide band of a range of rock types in Baltistan.

Correlation between Ladakh and southwestern Tibet is somewhat complicated by faulting and shearing as well as sparse data. The Ladakh batholith continues east across the KF into Tibet as a broad arc known as the Transhimalaya (Gangdese) batholith. The Ladakh batholith is cut by the KF, which displaces its original arc by approximately 150 km (Searle 1996). The Karakoram leucogranite, trending at a high angle to the KF in Pakistan, turns to become parallel to the KF in the Nubra valley. It follows the north side of the fault for approximately 150 km and then deviates from it to follow the more westerly regional trend, south of the Chang Chenmo River and north of the Pangong Lake (see Fig. 1a). Its easternmost limit is unknown at present. It is important to notice that both the Ladakh batholith and Karakoram leucogranite become parallel to the KF, the former running on its southern side and the latter on its northern side.

We have found no ophiolite remnants within the narrow deformation corridor separating the Ladakh and Karakoram batholiths, suggesting that the KF cuts across the suture zone. The Shyok Suture Zone counterpart in Tibet is the Pangong (Bangong)–Nujiang Suture Zone (Searle 1996). It crops out immediately south of the eastern Pangong Lake (e.g. Ratschbacher *et al.* 1994; Matte *et al.* 1996) and forms a long belt which can be followed to Amdo, 1200 km to the east. This suture zone is the first suture zone north of the Indus Suture Zone and separates the Changtang and Lhasa blocks. Near Amdo, fossil dating in the sediments transgressing the suture zone suggests that suturing occurred in the late Jurassic–early Cretaceous age (Girardeau *et al.*

1984), considerably earlier than the estimated suturing time in Kohistan (100–80 Ma). In Searle *et al.* (1998), we estimated that dextral movement on the KF was approximately 150 km by determining the southernmost outcrop of Karakoram leucogranites on the NE side of the fault and matching it to the southernmost outcrop of leucogranite on the SW side. Roughly the same value is found for the displacement of the Ladakh batholith. However, the fact that the two batholiths deviate from their regional trend to run parallel to the KF must imply that they were deformed internally, and not simply cut across by the fault. Interestingly, moving the fault back by 150 km, the Pangong–Nujiang Suture Zone becomes juxtaposed to the Saltoro Range, the expected location of the SSZ. Future work should concentrate on mapping the Saltoro Range, and the internal deformation of these two granite belts.

Conclusion

Regional tectonic reconstructions require a suture zone between the Kohistan–Dras arcs and the southern margin of Eurasia. We have not found evidence of this suture zone in the confluence area. Neither the Shyok Fm. nor the Nubra Fm., previously described as dismembered ophiolitic sequences, bear any evidence of including ophiolites. The former, with its graded-bedded sandstones interlayered with basalts, is probably part of the Dras island arc, whereas the metavolcanic rocks (including dacites) and metapelites of the latter represent the disrupted country rock of the Karakoram batholith and not a dismembered ophiolite sequence. The Khalsar Thrust shears rocks that can be directly linked in the field with the Shyok Fm. and Ladakh granitoids. North of the KT, in the southern slopes of the Saltoro Range, Srimal (1986*b*) and Srimal *et al.* (1987) described the Biagdang ophiolitic sequence. We have presented some observations that cast some doubt on that interpretation. An alternative location for the SSZ is the northern part of the Saltoro Range or along the Saltoro River. The presence of 60 ± 10 Ma granitoids north and south of the KT and KF suggests that the Dras–Kohistan island arc was already accreted to Eurasia by that time. The KF initiated after intrusion of the Karakoram leucogranite at 18–15 Ma. Movement on this young fault has juxtaposed the Ladakh and Saltoro blocks to the Karakoram terrane and thus the KF marks a terrane boundary. Vector analysis, using structural data from the KT and the two domains of the KF (KF–Nubra and –Shyok), suggests that these faults may be contemporaneous and kinematically linked. If this is so, oblique movement recorded by the N40–50W KF–Shyok is partitioned to thrusting along the N60W-striking KT and dextral strike-slip along the N30W-striking KF–Nubra. By removing 150 km of dextral displacement accumulated on the KF, the main trend of the Karakoram leucogranite and Ladakh (Transhimalaya) batholith become continuous across the fault, and the Pangong (Bangong)–Nujiang Suture Zone is moved roughly to the expected location of the Shyok Suture Zone.

We would like to thank the support provided by Profs D. Green and I. McDougall and Dr R. Griffiths. We would like to thank Simon Lamb for discussions on vector analysis and Mike Searle and Peter Molnar for discussion on the Karakoram Fault and field assistance. We would also like to thank careful and enlightened reviews of the paper by Mike Petterson and Asif Khan. RFW would also like to acknowledge the financial support of a European Community grant ERBFMBICT960583.

References

ALLÈGRE, C. J., CORTILLOT, V., TAPPONIER, P. & 31 OTHERS. 1984. Structure and evolution of the Himalaya–Tibet orogenic belt. *Nature*, **307**, 17–22.

ALLEN, T. & CHAMBERLAIN, P. C. 1991. Petrologic constraints on the tectonic history of the northern Shyok suture and the main Karakorum Thrust, Baltistan, Northern Pakistan. *Journal of Metamorphic Geology*, **9**, 403–418.

BECK, R. A., BURBANK, D. W., SERCOMBE, W. J. & 11 OTHERS. 1995. Stratigraphic evidence for an early collision between northwest India and Asia. *Nature*, **373**, 55–58.

BOSSART, P. & OTTIGER, R. 1989. Rocks of the Muree formation in northern Pakistan: indicators of a descending foreland basin of late Paleocene to middle Eocene age. *Eclogae Geologicae Helvetiae*, **82**, 133–165.

BROOKFIELD, M. E. & REYNOLDS, P. H. 1981. Late Cretaceous emplacement of the Indus suture zone ophiolitic melange and an Eocene–Oligocene magmatic arc on the northern edge of the Indian plate. *Earth and Planetary Science Letters*, **55**, 157–162.

—— & REYNOLDS, P. H. 1990. Miocene 40Ar/39Ar ages from the Karakoram Batholith and Shyok Mélange, northern Pakistan, indicate late Tertiary uplift and southward displacement. *Tectonophysics*, **172**, 155–167.

CLAOUÉ-LONG, J. C., COMPSTON, W., ROBERTS, J. & FANNING, C. M. 1995. Two Carboniferous ages: a comparison of SHRIMP zircon dating with conventional zircon ages and 40Ar/39Ar analysis. *In:* BERGGREN, W. A., KENT, D. V., AUBRY, M.-P. & HARDENBOL, J. (eds) *Geochronology Time*

Scales and Global Stratigraphic Correlation. Society for Sedimentary Geology, Special Publications, 3–21.

COWARD, M. P., BROUGHTON, R. D., LUFF, I. W., PETTERSON, M. G., PUDSEY, C. J., REX, D. C. & KHAN, M. A. 1986. Collision tectonics in the NW Himalayas. *In*: COWARD, M. P. & RIES, A. C. (eds) *Collision Tectonics.* Geological Society, London, Special Publications, **19**, 203–219.

DAINELLI, G. 1933–1934. *La Serei dei Terreni, Spedizione Italiana De Filippi 1913–1914, Ser. II, Vol. 2, Parte I, II.*

DE TERRA, H. 1932. *Geologische forschungen im westlichen K'un-Lun und Karakorum-Himalaya,* in *Wissenschaftliche ergebnisse der Dr Trinkler schen Zentralasien-expedition.* Dietricht Reimer.

DEBON, F. 1995. Incipient India–Eurasia collision and plutonism: the Lower Cenozoic Batura granites (Hunza Karakorum, North Pakistan). *Journal of the Geological Society, London*, **152**, 785–795.

FISCHER, F., OBERLI, F. & MEIER, M. 1989. Zircon dating of Oligocene and Miocene bentonites by the U–Pb method. *EUG V Abstracts Volume*, 419.

GAETANI, M., GARZANTI, E., JADOUIL, F., NICORA, A., TINTORI, A., PASINI, M. & KHAN, K. S. A. 1990. The north Karakorum side of the Central Asia geopuzzle. *Geological Society of America, Bulletin*, **102**, 54–62.

GANSSER, A. 1980. The division between Himalaya and Karakorum. *Geological Bulletin, University of Peshawar, Special Issue*, **13**, 9–22.

GIRARDEAU, J., MARCOUX, J., ALLEGRE, C. J., BASSOULLET, J. P., YOUKING, T., *et al.* 1984. Tectonic environment and geodynamic significance of the Neo-Cimmerian Donqiao ophiolite, Bangong–Nujiang suture zone, Tibet. *Nature*, **307**, 27–31.

HANSON, C. R. 1989. The northern suture in the Shigar valley, Baltistan, northern Pakistan. *In*: MALINCONICO, L. L. & LILLIE, R. J. (eds) *Tectonics of the Western Himalaya.* Geological Society of America, Special Paper, **232**, 203–215.

HEDIN, S. 1907. *Scientific results of a journey in Central Asia 1899–1902, Vol. VI–2 Geology*, Lithographic Institute of the General Staff of the Swedish Army, Stockholm.

HONEGGER, K., DIETRICH, V., FRANK, W., GANSSER, A., THÖNI, M. & TROMMSDORFF, V. 1982. Magmatism and metamorphism in the Ladakh Himalayas (the Indus–Tsangpo suture zone). *Earth and Planetary Science Letters*, **60**, 253–292.

LEMENNICIER, Y., LE FORT, P., LOMBARDO, B., PÊCHER, A. & ROLFO, F. 1996. Tectonometamorphic evolution of the central Karakorum (Baltistan, northern Pakistan). *Tectonophysics*, **260**, 119–143.

LOVERA, O. M. R., GROVE, M., HARRISON, T. M. & MAHON, K. I. 1997. Systematic analysis of K-feldspar $^{40}Ar/^{39}Ar$ step heating results. I. Significance of activation energy determination. *Geochimica et Cosmochimica Acta*, **61**, 3171–3192.

——, RICHTER, F. M. & HARRISON, T. M. 1989. $^{40}Ar/^{39}Ar$ thermochronology for slowly cooled samples having a distribution of diffusion domain sizes. *Journal of Geophysical Research*, **94**, 17917–17936.

MATTE, P., TAPPONNIER, P., ARNAUD, N., BOURJOT, L., AVOUAC, J. P. *et al.* 1996. Tectonics of Western Tibet, between Tarim and the Indus. *Earth and Planetary Science Letters*, **142**, 311–330.

MOLNAR, P. & TAPPONNIER, P. 1975. Cenozoic tectonics of Asia, effects of a continental collision. *Science*, **189**, 419–426.

PARRISH, R. R. & TIRRUL, R. 1989. U–Pb age of the Baltoro granite, northwest Himalaya, and implications for monazite U–Pb systematics. *Geology*, **17**, 1076–1079.

PELTZER, G. & TAPPONNIER, P. 1988. Formation and evolution of strike-slip faults, rifts, and basins during the India–Asia collision: an experimental approach. *Journal of Geophysical Research*, **93**, 15085–15117.

PETTERSON, M. G. & WINDLEY, B. F. 1985. Rb–Sr dating of the Kohistan arc-batholith in the Trans-Himalaya of north Pakistan, and tectonic implications. *Earth and Planetary Science Letters*, **74**, 45–57.

—— & —— 1991. Changing source regions of magmas and crustal growth in the Trans-Himalayas: evidence from the Chalt volcanics and Kohistan batholith, Kohistan, northern Pakistan. *Earth and Planetary Science Letters*, **102**, 326–341.

—— & —— 1992. The field relationships, geochemistry and petrogenesis of the Cretaceous basalt Jutal dyke suite, Kohistan, N. Pakistan. *Journal of the Geological Society, London*, **149**, 107–114.

——, —— & LUFF, I. W. 1990. The Chalt volcanics, Kohistan, Pakistan, high-Mg tholeiitic and low-Mg calc-alkaline volcanism in a Cretaceous island arc. *Physics and Chemistry of the Earth*, **17**, 19–30.

PUDSEY, C. J. 1986. The Northern Suture, Pakistan: margin of a Cretaceous island arc. *Geological Magazine*, **123**, 405–423.

RAI, H. 1982. Geological evidence against the Shyok palaeo-suture, Ladakh Himalaya. *Nature*, **297**, 142–144.

RATSCHBACHER, L., FRISCH, W., LIU, G. & CHEN, C. 1994. Distributed deformation in southern and western Tibet during and after the India–Asia collision. *Journal of Geophysical Research*, **99**, 19917–19945.

RAZ, U. & HONEGGER, K. 1989. Magmatic and tectonic evolution of the Ladakh Block from field studies. *Tectonophysics*, **161**, 107–118.

ROWLEY, D. B. 1996. Age of initiation of collision between India and Asia: a review of stratigraphic data. *Earth and Planetary Science Letters*, **145**, 1–13.

SCHÄRER, U., COPELAND, P., HARRISON, T. M. & SEARLE, M. P. 1990. Age, cooling history and origin of post-collisional leucogranites in the Karakoram batholith: A multi system isotope study of north Pakistan. *Journal of Geology*, **98**, 233–251.

——, HAMET, J. & ALLÈGRE, C. J. 1984. The Transhimalaya (Gangdese) plutonism in the Ladakh region: U–Pb and Rb–Sr study. *Earth and Planetary Science Letters*, **67**, 327–339.

SEARLE, M. P. 1991. *Geology and tectonics of the Karakoram mountains*. John Wiley & Sons, Chichester.

—— 1996. Geological evidence against large-scale pre-Holocene offsets along the Karakoram Fault: Implications for the limited extrusion of the Tibetan plateau. *Tectonics*, **15**, 171–186.

——, CRAWFORD, M. B. & REX, A. J. 1992. Field relations, geochemistry, origin and emplacement of the Baltoro granite, Central Karakoram. *Transactions of the Royal Society of Edinburgh: Earth Sciences*, **83**, 519–538.

——, REX, A. J., TIRRUL, R., REX, D. C. & BARNICOAT, A. 1989. Metamorphic, magmatic and tectonic evolution of the Central Karakoram in the Biafo–Baltoro–Hushe regions of N. Pakistan. *In*: MALINCONICO, L. L. & LILLIE, R. J. (eds) *Tectonics of the Western Himalayas*. Geological Society of America, Special Paper, **232**, 47–74.

——, WEINBERG, R. F. & DUNLAP, W. J. 1998. Transpressional tectonics along the Karakoram Fault Zone, northern Ladakh. *In*: HOLDSWORTH, R. E. & STRACHAN, R. A. (eds) *Continental Transpressional and Transtensional Tectonics*. Geological Society, London, Special Publications, **135**, 307–326.

SHARMA, K. K. & KUMAR, S. 1978. Contribution to the geology of Ladakh, north western Himalaya. *Himalayan Geology*, **8**, 252–287.

SRIMAL, N. 1986*a*. *Geology and oxygen and $^{40}Ar/^{39}Ar$ isotopic study of India–Asia collision in the Ladakh and Karakoram Himalaya, NW India*. PhD thesis, University of Rochester.

—— 1986*b*. India–Asia collision: implications from the geology of the eastern Karakoram. *Geology*, **14**, 523–527.

——, BASU, A. R. & KYSER, T. K. 1987. Tectonic inferences from oxygen isotopes in volcano-plutonic complexes of the India–Asia collision zone, NW India. *Tectonics*, **6**, 261–273.

STACEY, J. S. & KRAMERS, J. D. 1975. Approximation of terrestrial lead isotope evolution by a two-stage model. *Earth and Planetary Science Letters*, **26**, 207–221.

SULLIVAN, M. A., WINDLEY, B. F., SAUNDERS, A. D., HAYNES, J. R. & REX, D. C. 1993. A palaeogeographic reconstruction of the Dir Group: Evidence for magmatic arc migration within Kohistan, N. Pakistan. *In*: TRELOAR, P. J. & SEARLE, M. P. (eds) *Himalayan Tectonics*. Geological Society, London, Special Publications, **74**, 139–160.

TAHIRKHELI, R. A. K., MATTAUER, M., PROUST, F. & TAPPONNIER, P. 1979. The India–Eurasia suture zone in northern Pakistan, some new data for an interpretation of plate scale. *In*: FARAH, A. & DEJONG, K. A. (eds) *Geodynamics of Pakistan*. Geological Survey of Pakistan, Quetta, 125–130.

THAKUR, V. C. & MISRA, D. K. 1984. Tectonic framework of the Indus and Shyok suture zones in eastern Ladakh, northwest Himalaya. *Tectonophysics*, **101**, 207–220.

——, VIRDI, N. S., RAI, H. & GUPTA, K. R. 1981. A note on the geology of Nubra–Shyok area of Ladakh, Kashmir, Himalaya. *Journal of the Geological Society of India*, **22**, 46–50.

TRELOAR, P. J., GUISE, P. G., COWARD, M. P., SEARLE, M. P., WINDLEY, B. F. *et al.* 1989. K–Ar and Ar–Ar geochronology of the Himalayan collision in NW Pakistan: constraints on the timing of suturing, deformation, metamorphism and uplift. *Tectonics*, **8**, 881–909.

——, PETTERSON, M. G., JAN, M. Q. & SULLIVAN, M. A. 1996. A re-evaluation of the stratigraphy and evolution of the Kohistan arc sequence, Pakistan Himalaya: implications for magmatic and tectonic arc-building processes. *Journal of the Geological Society, London*, **153**, 681–693.

WEINBERG, R. F. 1997. The disruption of a diorite magma pool by intruding granite: the Sobu body, Ladakh Batholith, Indian Himalayas. *Journal of Geology*, **105**, 87–98.

—— & DUNLAP, W. J. in press. Growth and deformation of the Ladakh Batholith, NW Himalayas: implications for timing of continental collision and origin of calc-alkaline batholiths. *Journal of Geology*.

WHITEHOUSE, M. J., CLAESSON, S., SUNDE, T. & VESTIN, J. 1997. Ion-microprobe U–Pb zircon geochronology and correlation of Archaean gneisses from the Lewisian Complex of Gruinard Bay, northwest Scotland. *Geochimica et Cosmochimica Acta*, **61**, 4429–4438.

WIEDENBECK, M., ALLÉ, P., CORFU, F., GRIFFIN, W. L., MEIER, M. *et al.* 1995. Three natural zircon standards for U–Th–Pb, Lu–Hf, trace element and REE analysis. *Geostandards Newsletter*, **19**, 1–23.

ZECK, H. P. & WHITEHOUSE, M. J. in press. Hercynian, Pan-African, Proterozoic and Archean ion-microprobe zircon ages for a Betic–Rift core complex, Alpine belt, W. Mediterranean-consequences for its P–T–t path. *Contributions to Mineralogy and Petrology*.